

An exact 3D solution for free vibrations of multilayered cross-ply composite and sandwich plates and shells

*Original*

An exact 3D solution for free vibrations of multilayered cross-ply composite and sandwich plates and shells / Brischetto, Salvatore. - In: INTERNATIONAL JOURNAL OF APPLIED MECHANICS. - ISSN 1758-8251. - 6:6(2014), pp. 1-42. [10.1142/S1758825114500768]

*Availability:*

This version is available at: 11583/2580141 since: 2020-06-03T23:52:46Z

*Publisher:*

World Scientific Publishing

*Published*

DOI:10.1142/S1758825114500768

*Terms of use:*

This article is made available under terms and conditions as specified in the corresponding bibliographic description in the repository

*Publisher copyright*

(Article begins on next page)

# An exact three-dimensional solution for free vibrations of multilayered composite and sandwich plates and shells

Salvatore Brischetto\*

## Abstract

*A three-dimensional free vibration analysis of multilayered structures is proposed. The exact solution is developed for the differential equations of equilibrium written in general orthogonal curvilinear coordinates. The equations consider a geometry for shells without simplifications and allow the analysis of spherical shell panels, cylindrical shell panels, cylindrical closed shells and plates. The method is based on a layer-wise approach, the continuity of displacements and transverse shear/normal stresses is imposed at the interfaces between the layers of the structures. Results are given for multilayered composite and sandwich plates and shells. A free vibration analysis is proposed for a number of vibration modes, thickness ratios, imposed wave numbers, geometries and multilayer configurations embedding isotropic and orthotropic composite materials. These results can also be used as reference solutions for plate and shell two-dimensional models developed for the analysis of multilayered structures.*

**Keywords:** multilayered structures, composite structures, sandwich structures, plates, shells, three-dimensional elastic analysis, exact solution, free vibrations, vibration modes.

## 1 Introduction

The application of composite materials and sandwich configurations in aircraft, spacecraft, ship, and automotive vehicle structures has increased rapidly over the past three decades. Composite materials offer many advantages with respect to traditional metallic ones because of their high strength and low weight. Sandwich configurations are used to provide a stronger and stiffer structure for the same weight, or conversely lighter structures to carry the same load as a homogenous or compact-laminate element. A number of complicating effects arises in the design, analysis, modeling and manufacturing of composite and sandwich structures. The development of plate and shell elements is fundamental for the analysis of these multilayered structures. For this reason, plate and shell elements need accurate validation. Three-dimensional exact solutions allow such validations and checks to be made. These solutions also give further details about three-dimensional behavior and complicating effects introduced by these new configurations, e.g, the coupling between shear and axial strains (due to the in-plane anisotropy) and the zigzag form of displacements through the thickness and interlaminar continuity (due to the transverse anisotropy). In the literature, works about exact three-dimensional solutions do not give a general overview of plate and shell elements because they analyze the various geometries separately. The present paper aims to fill this gap by proposing a general formulation for the equations

---

\*Corresponding author: Salvatore Brischetto, Department of Mechanical and Aerospace Engineering, Politecnico di Torino, Corso Duca degli Abruzzi, 24, 10129 Torino, ITALY. tel: +39.011.090.6813, fax: +39.011.090.6899, e.mail: salvatore.brischetto@polito.it.

of motion in orthogonal curvilinear coordinates that is valid for multilayered square and rectangular plates, cylindrical shell panels, spherical shell panels and cylinders. This formulation is an extension of the one-layered cases shown in the companion paper [1]. The present paper exactly solves the equations of motion in general curvilinear orthogonal coordinates including an exact geometry for shell structures without simplifications. The method uses a layer-wise approach that imposes the continuity of displacements and transverse shear/normal stresses at the interfaces between layers embedded in the multilayered plates and shells.

Three-dimensional analysis of plates are usually performed by using equations in orthogonal rectangular coordinates. These equations do not allow the analysis of shell geometries. Pagano [2] proposed three-dimensional elasticity solutions for rectangular laminates with pinned edges. Several specific example problems were solved (including a sandwich plate), and comparisons with classical laminated plate theory were also given. The elasticity solution for sandwich structural elements such as beams, orthotropic plates and shells was considered in [3]. Results were given for the plate case only. However, Meyer-Piening [3] considers that the analysis has the potential to be extended to curved shell panels. Analytical three-dimensional solutions for free vibrations of a simply supported rectangular plate made of an incompressible homogeneous linear elastic isotropic material were proposed in [4] and [5]. Some frequencies missing in previous analytical solutions were also identified here. A three-dimensional linear elastic, small deformation theory obtained by the direct method was developed in [6] for the free vibration of simply supported, homogeneous, isotropic, thick rectangular plates. The same method was also proposed in [7] for the flexure of simply supported homogeneous, isotropic, thick rectangular plates under arbitrary loading. The expansion in terms of infinite series was formally exact and yielded accurate numerical results without undue effort. Batra et al. [8] showed useful comparisons between two-dimensional models and an exact three-dimensional solution for the free vibrations of a simply supported rectangular orthotropic thick plate. Ye [9] presented a three-dimensional elastic free vibration analysis of cross-ply laminated rectangular plates with clamped boundaries, the analysis was based on a recursive solution. Comparisons between 2D-displacement-based-models and exact results of the linear three-dimensional elasticity were proposed in [10] for natural frequencies, displacement and stress quantities in multilayered plates. A global three-dimensional Ritz formulation was employed in [11] for the exact three-dimensional elastic investigation of isosceles triangular plates, and in [12] for the three-dimensional elastic free vibration analysis of a circular plate. A set of orthogonal polynomial series was used to approximate the spatial displacements. Theoretical high frequency vibration analysis is fundamental in a variety of engineering designs. The importance of high frequency analysis of multilayered composite plates was also confirmed in the literature. Zhao et al. [13] introduced the discrete singular convolution (DSC) algorithm for high frequency vibration analysis of plate structures, the Levy method was also employed to provide exact solutions to validate the DSC algorithm. The same investigation (comparison between DSC algorithm and the Levy method) was also proposed in [14]. Taher et al. [15] computed the first nine frequency parameters of circular and annular plates with variable thickness and combined boundary conditions, the eigenvalue equation was derived by means of three-dimensional elasticity theory and Ritz method. Xing and Liu [16] proposed the separation of variables to solve the Hamiltonian dual form of eigenvalue problem for transverse free vibrations of thin plates. The extension of 3D exact analysis to functionally graded plates was performed in [17]-[19] for free vibrations, forced vibrations and displacement and stress analysis under static loads. The extension of three-dimensional solutions to plates embedding piezoelectric layers was given in [20]-[25] for static, bending, free vibration and steady state harmonic responses. In [20]-[25] an exact three-dimensional distribution of mechanical and electric quantities in inhomogeneous and laminated piezoelectric plates is proposed in the framework of linear theory of piezoelectricity.

The most relevant works about three-dimensional shell analysis were discussed in [26]-[42]. The coupled free vibrations of a transversely isotropic cylindrical shell embedded in an elastic medium were studied in [26] where the three-dimensional elastic solution used three displacement functions to rep-

resent the three displacement components. Fan and Zhang [27] showed static, dynamic and buckling three-dimensional analysis of thick open laminated cylindrical shells by means of the Cayley-Hamilton theorem. The state equation for orthotropy was established in a cylindrical coordinate system. Free vibrations of simply-supported cylindrical shells were studied in [28] on the basis of three dimensional exact theory. Extensive frequency parameters were obtained by solving frequency equations. The free vibrations of simply-supported cross-ply cylindrical and doubly-curved laminates were investigated in [29]. The three-dimensional equations of motion were reduced to a system of coupled ordinary differential equations and then solved using the power series method. The three-dimensional free vibrations of a homogenous isotropic, viscothermoelastic hollow sphere were studied in [30]. The surfaces were subjected to stress-free, thermally insulated or isothermal boundary conditions. The exact three-dimensional vibration analysis of a trans-radially isotropic, thermoelastic solid sphere was analyzed in [31]. The governing partial differential equations in [30] and [31] were solved into a coupled system of ordinary differential equations. Fröbenius matrix method was employed to obtain the solution. Soldatos and Ye [32] proposed exact, three-dimensional, free vibration analysis of angle-ply laminated thick cylinders having a regular symmetric or a regular antisymmetric angle-ply lay-up. Armenakas et al. [33] proposed a self-contained treatment of the problem of plane harmonic waves propagation along a hollow circular cylinder in the framework of the three-dimensional theory of elasticity. A comparison between a refined two-dimensional analysis, a shear deformation theory, the Flügge theory and an exact elasticity analysis was proposed in [34] for frequency investigation. Further details about the Flügge classical thin shell theory concerning the free vibrations of cylindrical shells with elastic boundary conditions can be found in [35]. Other comparisons between two-dimensional closed form solutions and available exact 3-D elastic and analytical solutions for the free vibration analysis of simply supported and clamped homogenous isotropic circular cylindrical shells were also proposed in [36]. Vel [37] extended exact elasticity solutions to functionally graded cylindrical shells. The three-dimensional linear elastodynamics equations were solved using suitable displacement functions that identically satisfy the boundary conditions. Loy and Lam [38] obtained the governing equation using an energy minimization principle. A layer-wise approach was proposed to study the vibration of thick circular cylindrical shells on the basis of three-dimensional theory of elasticity. Wang et al. [39] proposed the three-dimensional free vibration analysis of magneto-electro-elastic cylindrical panels. Further results about three-dimensional analysis of shells, where the solutions are not given in closed form, can be found in [40] for the dynamic stiffness matrix method and in [41] and [42] for the three-dimensional Ritz method for vibration of spherical shells.

The papers in the literature show the three-dimensional analysis of plates or shells. They include static and dynamic analysis, functionally graded materials, composite and piezoelectric materials, displacement and mixed models. The novelty introduced by the present paper is the general formulation for all the geometries (square and rectangular plates, cylindrical and spherical shell panels, and cylindrical closed shells). The equations of motion for the dynamic case are written in general orthogonal curvilinear coordinates using an exact geometry for multilayered shells. The system of second order differential equations is reduced to a system of first order differential equations, and afterwards it is exactly solved using the exponential matrix method and the Navier-type solution. The approach is developed in layer-wise form by imposing the continuity of displacements and transverse shear/normal stresses at each interface. The exponential matrix method has already been used in [10] for the three-dimensional analysis of plates in rectilinear orthogonal coordinates and in [32] for an exact, three-dimensional, free vibration analysis of angle-ply laminated cylinders in cylindrical coordinates. The equations of motion written in orthogonal curvilinear coordinates are a general form of the equations of motions written in rectilinear orthogonal coordinates in [10] and in cylindrical coordinates in [32]. These equations allow general exact solutions for multilayered plate and shell geometries as already done in the one-layered plate and shell cases proposed in [1].

Section 2 gives equations of motion in general orthogonal curvilinear coordinates for dynamic analysis

of plates and shells. Section 3 shows geometrical relations and three-dimensional constitutive equations for spherical shells by means of an exact geometrical approach. These equations automatically degenerate into geometrical relations for cylindrical shells and plates. Section 4 gives the closed form solution of equations of motion and their multilayer extension. Vibration modes related to frequency values are obtained from the same system of equations. Section 5 shows results, the method is validated by means of three preliminary assessments for multilayered composite square plate, cylindrical shell and spherical shell. The geometries for the new benchmarks are square and rectangular plates, cylinders, cylindrical and spherical shell panels. Each structure is analyzed as a sandwich configuration with an isotropic foam core and external skins that can be made of isotropic aluminium alloy or multilayered composite layers. The free vibration analysis considers the effects of materials, angle of orthotropy, thickness ratios, imposed wave numbers, order of frequencies and vibration modes. Conclusions are discussed in Section 6.

## 2 Equilibrium equations in orthogonal curvilinear coordinates

A shell is a three-dimensional body bounded by two closely spaced curved surfaces where one dimension (the distance between the two surfaces) is small in comparison with the other two dimensions in the plane directions. The distance between the surfaces measured along the normal to the middle surface is the *thickness* of the shell at that point [43], [44]. The middle surface  $\Omega_0$  of the shell is the locus of points which lie midway between these surfaces. Geometry and the reference system are indicated in Fig. 1 where curvilinear orthogonal coordinates  $(\alpha, \beta, z)$  are shown. Displacement components are  $u$ ,  $v$ , and  $w$  in  $\alpha$ ,  $\beta$  and  $z$  directions, respectively. The square of an infinitesimal linear segment in the layer is:

$$ds^2 = g_1 d\alpha^2 + g_2 d\beta^2 + g_3 dz^2, \quad (1)$$

where

$$g_1 = H_\alpha^2 = [A(1 + \frac{z}{R_\alpha})]^2, \quad g_2 = H_\beta^2 = [B(1 + \frac{z}{R_\beta})]^2, \quad g_3 = H_z^2 = 1. \quad (2)$$

The quantities  $g_1$ ,  $g_2$ ,  $g_3$ ,  $A$ ,  $B$ ,  $R_\alpha$ ,  $R_\beta$  are connected by the equations of Lamb [44] because the three-dimensional space where the three independent variables  $\alpha$ ,  $\beta$  and  $z$  vary is an Euclidean space.  $R_\alpha$  and  $R_\beta$  are the principal radii of curvature along the coordinates  $\alpha$  and  $\beta$ , respectively.  $A$  and  $B$  are the coefficients of the first fundamental form of the surface  $\Omega_0$ ,  $z$  is the thickness coordinate that varies from  $-h/2$  to  $+h/2$  (where  $h$  is the thickness of the structure as shown in Fig. 1).  $g_3 = 1$  because  $z$  is a rectilinear coordinate.

The fundamental shell element is the differential element bounded by two surfaces  $dz$  apart at a distance  $z$  from the middle surface and four ruled surfaces whose generators are the normals to the middle surface along the parametric curves  $\alpha = \alpha_0$ ,  $\alpha = \alpha_0 + d\alpha$ ,  $\beta = \beta_0$  and  $\beta = \beta_0 + d\beta$  [44]. The lengths of the edges of this fundamental element are (see Fig. 1):

$$\begin{aligned} ds_\alpha(z) &= A(1 + z/R_\alpha) d\alpha, \\ ds_\beta(z) &= B(1 + z/R_\beta) d\beta, \end{aligned} \quad (3)$$

the differential areas of the edge faces of the fundamental element are (see Fig. 1):

$$\begin{aligned} dA_\alpha(z) &= A(1 + z/R_\alpha) d\alpha dz, \\ dA_\beta(z) &= B(1 + z/R_\beta) d\beta dz, \end{aligned} \quad (4)$$

the associated infinitesimal area is:

$$d\Omega(z) = [A(1 + z/R_\alpha)][B(1 + z/R_\beta)] d\alpha d\beta, \quad (5)$$

and the volume of the fundamental element is:

$$dV(z) = [A(1 + z/R_\alpha)][B(1 + z/R_\beta)]d\alpha d\beta dz. \quad (6)$$

The parametric coefficients for shells with constant radii of curvature ( $A=B=1$ ) are:

$$H_\alpha = (1 + \frac{z}{R_\alpha}) = (1 + \frac{\tilde{z} - h/2}{R_\alpha}), \quad H_\beta = (1 + \frac{z}{R_\beta}) = (1 + \frac{\tilde{z} - h/2}{R_\beta}), \quad H_z = 1, \quad (7)$$

$H_\alpha$  and  $H_\beta$  depend on  $z$  or  $\tilde{z}$  coordinate (see Fig.2).

The three differential equations of equilibrium written for the case of free vibration analysis of multilayered spherical shells made of  $N_L$  layers with constant radii of curvature  $R_\alpha$  and  $R_\beta$  are here given (the most general form for variable radii of curvature can be found in [45] and [46]):

$$H_\beta \frac{\partial \sigma_{\alpha\alpha k}}{\partial \alpha} + H_\alpha \frac{\partial \sigma_{\alpha\beta k}}{\partial \beta} + H_\alpha H_\beta \frac{\partial \sigma_{\alpha z k}}{\partial z} + (\frac{2H_\beta}{R_\alpha} + \frac{H_\alpha}{R_\beta}) \sigma_{\alpha z k} = \rho_k H_\alpha H_\beta \ddot{u}_k, \quad (8)$$

$$H_\beta \frac{\partial \sigma_{\alpha\beta k}}{\partial \alpha} + H_\alpha \frac{\partial \sigma_{\beta\beta k}}{\partial \beta} + H_\alpha H_\beta \frac{\partial \sigma_{\beta z k}}{\partial z} + (\frac{2H_\alpha}{R_\beta} + \frac{H_\beta}{R_\alpha}) \sigma_{\beta z k} = \rho_k H_\alpha H_\beta \ddot{v}_k, \quad (9)$$

$$H_\beta \frac{\partial \sigma_{\alpha z k}}{\partial \alpha} + H_\alpha \frac{\partial \sigma_{\beta z k}}{\partial \beta} + H_\alpha H_\beta \frac{\partial \sigma_{zz k}}{\partial z} - \frac{H_\beta}{R_\alpha} \sigma_{\alpha\alpha k} - \frac{H_\alpha}{R_\beta} \sigma_{\beta\beta k} + (\frac{H_\beta}{R_\alpha} + \frac{H_\alpha}{R_\beta}) \sigma_{zz k} = \rho_k H_\alpha H_\beta \ddot{w}_k, \quad (10)$$

where  $\rho_k$  is the mass density,  $(\sigma_{\alpha\alpha k}, \sigma_{\beta\beta k}, \sigma_{zz k}, \sigma_{\beta z k}, \sigma_{\alpha z k}, \sigma_{\alpha\beta k})$  are the six stress components and  $\ddot{u}_k, \ddot{v}_k$  and  $\ddot{w}_k$  indicate the second temporal derivative of the three displacement components. Each quantity depends on the  $k$  layer.  $R_\alpha$  and  $R_\beta$  are referred to the mid-surface  $\Omega_0$  of the whole multilayered shell.  $H_\alpha$  and  $H_\beta$  continuously vary through the thickness of the multilayered shell and depend on the thickness coordinate.

### 3 Geometrical and constitutive relations

The strain-displacement relations of three-dimensional theory of elasticity in orthogonal curvilinear coordinates, as also shown in [45] and [47], are written for the generic  $k$  layer of the multilayered shell:

$$\epsilon_{\alpha\alpha k} = \frac{1}{(1 + z/R_\alpha)} \left( \frac{1}{A} \frac{\partial u_k}{\partial \alpha} + \frac{v_k}{AB} \frac{\partial A}{\partial \beta} + \frac{w_k}{R_\alpha} \right), \quad (11)$$

$$\epsilon_{\beta\beta k} = \frac{1}{(1 + z/R_\beta)} \left( \frac{u_k}{AB} \frac{\partial B}{\partial \alpha} + \frac{1}{B} \frac{\partial v_k}{\partial \beta} + \frac{w_k}{R_\beta} \right), \quad (12)$$

$$\epsilon_{zz k} = \frac{\partial w_k}{\partial z}, \quad (13)$$

$$\gamma_{\alpha\beta k} = \frac{A(1 + z/R_\alpha)}{B(1 + z/R_\beta)} \frac{\partial}{\partial \beta} \left[ \frac{u_k}{A(1 + z/R_\alpha)} \right] + \frac{B(1 + z/R_\beta)}{A(1 + z/R_\alpha)} \frac{\partial}{\partial \alpha} \left[ \frac{v_k}{B(1 + z/R_\beta)} \right], \quad (14)$$

$$\gamma_{\alpha z k} = \frac{1}{A(1 + z/R_\alpha)} \frac{\partial w_k}{\partial \alpha} + A(1 + z/R_\alpha) \frac{\partial}{\partial z} \left[ \frac{u_k}{A(1 + z/R_\alpha)} \right], \quad (15)$$

$$\gamma_{\beta z k} = \frac{1}{B(1 + z/R_\beta)} \frac{\partial w_k}{\partial \beta} + B(1 + z/R_\beta) \frac{\partial}{\partial z} \left[ \frac{v_k}{B(1 + z/R_\beta)} \right], \quad (16)$$

symbol  $\partial$  indicates the partial derivatives. In this work, we will focus only to shells with constant radii of curvature (e.g., cylindrical and spherical geometries) for which  $A=B=1$ . The geometrical relations

in Eqs.(11)-(16) written for shells with constant radii of curvature are defined as:

$$\epsilon_{\alpha\alpha k} = \frac{1}{H_\alpha} \frac{\partial u_k}{\partial \alpha} + \frac{w_k}{H_\alpha R_\alpha} , \quad (17)$$

$$\epsilon_{\beta\beta k} = \frac{1}{H_\beta} \frac{\partial v_k}{\partial \beta} + \frac{w_k}{H_\beta R_\beta} , \quad (18)$$

$$\epsilon_{zzk} = \frac{\partial w_k}{\partial z} , \quad (19)$$

$$\gamma_{\alpha\beta k} = \frac{1}{H_\alpha} \frac{\partial v_k}{\partial \alpha} + \frac{1}{H_\beta} \frac{\partial u_k}{\partial \beta} , \quad (20)$$

$$\gamma_{\alpha z k} = \frac{1}{H_\alpha} \frac{\partial w_k}{\partial \alpha} + \frac{\partial u_k}{\partial z} - \frac{u_k}{H_\alpha R_\alpha} , \quad (21)$$

$$\gamma_{\beta z k} = \frac{1}{H_\beta} \frac{\partial w_k}{\partial \beta} + \frac{\partial v_k}{\partial z} - \frac{v_k}{H_\beta R_\beta} . \quad (22)$$

General geometrical relations for spherical shells degenerate into geometrical relations for cylindrical shells when  $R_\alpha$  or  $R_\beta$  is infinite (with  $H_\alpha$  or  $H_\beta$  equals one), and they degenerate into geometrical relations for plates when both  $R_\alpha$  and  $R_\beta$  are infinite (with  $H_\alpha=H_\beta=1$ ).

Three-dimensional linear elastic constitutive equations in orthogonal curvilinear coordinates ( $\alpha, \beta, z$ ) for orthotropic material in the structural reference system are given for a generic  $k$  layer of the multilayered structure:

$$\sigma_{\alpha\alpha k} = C_{11k}\epsilon_{\alpha\alpha k} + C_{12k}\epsilon_{\beta\beta k} + C_{13k}\epsilon_{zzk} + C_{16k}\gamma_{\alpha\beta k} , \quad (23)$$

$$\sigma_{\beta\beta k} = C_{12k}\epsilon_{\alpha\alpha k} + C_{22k}\epsilon_{\beta\beta k} + C_{23k}\epsilon_{zzk} + C_{26k}\gamma_{\alpha\beta k} , \quad (24)$$

$$\sigma_{zzk} = C_{13k}\epsilon_{\alpha\alpha k} + C_{23k}\epsilon_{\beta\beta k} + C_{33k}\epsilon_{zzk} + C_{36k}\gamma_{\alpha\beta k} , \quad (25)$$

$$\sigma_{\beta z k} = C_{44k}\gamma_{\beta z k} + C_{45k}\gamma_{\alpha z k} , \quad (26)$$

$$\sigma_{\alpha z k} = C_{45k}\gamma_{\beta z k} + C_{55k}\gamma_{\alpha z k} , \quad (27)$$

$$\sigma_{\alpha\beta k} = C_{16k}\epsilon_{\alpha\alpha k} + C_{26k}\epsilon_{\beta\beta k} + C_{36k}\epsilon_{zzk} + C_{66k}\gamma_{\alpha\beta k} . \quad (28)$$

Geometrical relations (Eqs.(17)-(22)) are inserted in constitutive equations (Eqs.(23)-(28)) and partial derivatives  $\frac{\partial}{\partial \alpha}$ ,  $\frac{\partial}{\partial \beta}$  and  $\frac{\partial}{\partial z}$  are indicated with subscripts  $_{,\alpha}$ ,  $_{,\beta}$  and  $_{,z}$ . A closed form solution of differential equations of equilibrium for shells are obtained when coefficients  $C_{16k}$ ,  $C_{26k}$ ,  $C_{36k}$  and  $C_{45k}$  are set to zero (this means orthotropic angle  $\theta$  equals  $0^\circ$  or  $90^\circ$ ):

$$\sigma_{\alpha\alpha k} = \frac{C_{11k}}{H_\alpha} u_{k,\alpha} + \frac{C_{11k}}{H_\alpha R_\alpha} w_k + \frac{C_{12k}}{H_\beta} v_{k,\beta} + \frac{C_{12k}}{H_\beta R_\beta} w_k + C_{13k} w_{k,z} , \quad (29)$$

$$\sigma_{\beta\beta k} = \frac{C_{12k}}{H_\alpha} u_{k,\alpha} + \frac{C_{12k}}{H_\alpha R_\alpha} w_k + \frac{C_{22k}}{H_\beta} v_{k,\beta} + \frac{C_{22k}}{H_\beta R_\beta} w_k + C_{23k} w_{k,z} , \quad (30)$$

$$\sigma_{zzk} = \frac{C_{13k}}{H_\alpha} u_{k,\alpha} + \frac{C_{13k}}{H_\alpha R_\alpha} w_k + \frac{C_{23k}}{H_\beta} v_{k,\beta} + \frac{C_{23k}}{H_\beta R_\beta} w_k + C_{33k} w_{k,z} , \quad (31)$$

$$\sigma_{\beta z k} = \frac{C_{44k}}{H_\beta} w_{k,\beta} + C_{44k} v_{k,z} - \frac{C_{44k}}{H_\beta R_\beta} v_k , \quad (32)$$

$$\sigma_{\alpha z k} = \frac{C_{55k}}{H_\alpha} w_{k,\alpha} + C_{55k} u_{k,z} - \frac{C_{55k}}{H_\alpha R_\alpha} u_k , \quad (33)$$

$$\sigma_{\alpha\beta k} = \frac{C_{66k}}{H_\alpha} v_{k,\alpha} + \frac{C_{66k}}{H_\beta} u_{k,\beta} . \quad (34)$$

## 4 Closed form of equilibrium equations

The first step is the substitution of the Eqs.(29)-(34) in Eqs.(8)-(10) to obtain a displacement form of the equilibrium relations. The following form of differential equations of equilibrium is given for a generic  $k$  layer:

$$\begin{aligned} & \left( -\frac{H_\beta C_{55k}}{H_\alpha R_\alpha^2} - \frac{C_{55k}}{R_\alpha R_\beta} \right) u_k + \left( \frac{C_{55k} H_\beta}{R_\alpha} + \frac{C_{55k} H_\alpha}{R_\beta} \right) u_{k,z} + \left( \frac{C_{11k} H_\beta}{H_\alpha} \right) u_{k,\alpha\alpha} + \left( \frac{C_{66k} H_\alpha}{H_\beta} \right) u_{k,\beta\beta} + \\ & \left( C_{55k} H_\alpha H_\beta \right) u_{k,zz} + \left( C_{12k} + C_{66k} \right) v_{k,\alpha\beta} + \left( \frac{C_{11k} H_\beta}{H_\alpha R_\alpha} + \frac{C_{12k}}{R_\beta} + \frac{C_{55k} H_\beta}{H_\alpha R_\alpha} + \frac{C_{55k}}{R_\beta} \right) w_{k,\alpha} + \end{aligned} \quad (35)$$

$$\begin{aligned} & \left( C_{13k} H_\beta + C_{55k} H_\beta \right) w_{k,\alpha z} = \rho_k H_\alpha H_\beta \ddot{u}_k, \\ & \left( -\frac{H_\alpha C_{44k}}{H_\beta R_\beta^2} - \frac{C_{44k}}{R_\alpha R_\beta} \right) v_k + \left( \frac{C_{44k} H_\alpha}{R_\beta} + \frac{C_{44k} H_\beta}{R_\alpha} \right) v_{k,z} + \left( \frac{C_{66k} H_\beta}{H_\alpha} \right) v_{k,\alpha\alpha} + \left( \frac{C_{22k} H_\alpha}{H_\beta} \right) v_{k,\beta\beta} + \\ & \left( C_{44k} H_\alpha H_\beta \right) v_{k,zz} + \left( C_{12k} + C_{66k} \right) u_{k,\alpha\beta} + \left( \frac{C_{44k} H_\alpha}{H_\beta R_\beta} + \frac{C_{44k}}{R_\alpha} + \frac{C_{22k} H_\alpha}{H_\beta R_\beta} + \frac{C_{12k}}{R_\alpha} \right) w_{k,\beta} + \end{aligned} \quad (36)$$

$$\begin{aligned} & \left( C_{44k} H_\alpha + C_{23k} H_\alpha \right) w_{k,\beta z} = \rho_k H_\alpha H_\beta \ddot{v}_k, \\ & \left( \frac{C_{13k}}{R_\alpha R_\beta} + \frac{C_{23k}}{R_\alpha R_\beta} - \frac{C_{11k} H_\beta}{H_\alpha R_\alpha^2} - \frac{2C_{12k}}{R_\alpha R_\beta} - \frac{C_{22k} H_\alpha}{H_\beta R_\beta^2} \right) w_k + \left( -\frac{C_{55k} H_\beta}{H_\alpha R_\alpha} + \frac{C_{13k}}{R_\beta} - \frac{C_{11k} H_\beta}{H_\alpha R_\alpha} - \frac{C_{12k}}{R_\beta} \right) u_{k,\alpha} + \\ & \left( -\frac{C_{44k} H_\alpha}{H_\beta R_\beta} + \frac{C_{23k}}{R_\alpha} - \frac{C_{22k} H_\alpha}{H_\beta R_\beta} - \frac{C_{12k}}{R_\alpha} \right) v_{k,\beta} + \left( \frac{C_{33k} H_\beta}{R_\alpha} + \frac{C_{33k} H_\alpha}{R_\beta} \right) w_{k,z} + \\ & \left( C_{55k} H_\beta + C_{13k} H_\beta \right) u_{k,\alpha z} + \left( C_{44k} H_\alpha + C_{23k} H_\alpha \right) v_{k,\beta z} + \left( C_{55k} \frac{H_\beta}{H_\alpha} \right) w_{k,\alpha\alpha} + \left( C_{44k} \frac{H_\alpha}{H_\beta} \right) w_{k,\beta\beta} + \\ & \left( C_{33k} H_\alpha H_\beta \right) w_{k,zz} = \rho_k H_\alpha H_\beta \ddot{w}_k. \end{aligned} \quad (37)$$

$R_\alpha$  and  $R_\beta$  refer to the reference mid-surface  $\Omega_0$  of the multilayered shell.  $H_\alpha$  and  $H_\beta$  are calculated through the thickness of the multilayered shell by means of Eq.(7). Equilibrium relations in Eqs.(35)-(37) are for spherical shell panels, they automatically degenerate into equilibrium equations for cylindrical closed/open shell panels [32] when  $R_\alpha$  or  $R_\beta$  is infinite (with  $H_\alpha$  or  $H_\beta$  equals one) and into equilibrium equations for plates [10] when  $R_\alpha$  and  $R_\beta$  are infinite (with  $H_\alpha$  and  $H_\beta$  equal one). In this way, a unique and general formulation is possible for any geometry.

The closed form of Eqs.(35)-(37) is obtained for simply supported shells and plates made of isotropic material or orthotropic material with  $0^\circ$  or  $90^\circ$  orthotropic angle (in both cases  $C_{16k} = C_{26k} = C_{36k} = C_{45k} = 0$ ). The three displacement components have the following harmonic form:

$$u_k = U_k(z) e^{i\omega t} \cos(\bar{\alpha}\alpha) \sin(\bar{\beta}\beta), \quad (38)$$

$$v_k = V_k(z) e^{i\omega t} \sin(\bar{\alpha}\alpha) \cos(\bar{\beta}\beta), \quad (39)$$

$$w_k = W_k(z) e^{i\omega t} \sin(\bar{\alpha}\alpha) \sin(\bar{\beta}\beta), \quad (40)$$

where  $U_k$ ,  $V_k$  and  $W_k$  are the displacement amplitudes in  $\alpha$ ,  $\beta$  and  $z$  directions, respectively.  $i$  is the coefficient of the imaginary unit,  $\omega = 2\pi f$  is the circular frequency where  $f$  is the frequency value,  $t$  is the time. In coefficients  $\bar{\alpha} = \frac{m\pi}{a}$  and  $\bar{\beta} = \frac{n\pi}{b}$ ,  $m$  and  $n$  are the half-wave numbers and  $a$  and  $b$  are the shell dimensions in  $\alpha$  and  $\beta$  directions, respectively (calculated in the mid-surface  $\Omega_0$ ).



Eqs.(38)-(40) are substituted in Eqs.(35)-(37) to obtain the following system of equations:

$$\begin{aligned} & \left( -\frac{C_{55k}H_\beta}{H_\alpha R_\alpha^2} - \frac{C_{55k}}{R_\alpha R_\beta} - \bar{\alpha}^2 \frac{C_{11k}H_\beta}{H_\alpha} - \bar{\beta}^2 \frac{C_{66k}H_\alpha}{H_\beta} + \rho_k H_\alpha H_\beta \omega^2 \right) U_k + \left( -\bar{\alpha}\bar{\beta}C_{12k} - \bar{\alpha}\bar{\beta}C_{66k} \right) V_k + \\ & \left( \bar{\alpha} \frac{C_{11k}H_\beta}{H_\alpha R_\alpha} + \bar{\alpha} \frac{C_{12k}}{R_\beta} + \bar{\alpha} \frac{C_{55k}H_\beta}{H_\alpha R_\alpha} + \bar{\alpha} \frac{C_{55k}}{R_\beta} \right) W_k + \left( \frac{C_{55k}H_\beta}{R_\alpha} + \frac{C_{55k}H_\alpha}{R_\beta} \right) U_{k,z} + \left( \bar{\alpha}C_{13k}H_\beta + \right. \\ & \left. \bar{\alpha}C_{55k}H_\beta \right) W_{k,z} + \left( C_{55k}H_\alpha H_\beta \right) U_{k,zz} = 0, \end{aligned} \quad (41)$$

$$\begin{aligned} & \left( -\bar{\alpha}\bar{\beta}C_{66k} - \bar{\alpha}\bar{\beta}C_{12k} \right) U_k + \left( -\frac{C_{44k}H_\alpha}{H_\beta R_\beta^2} - \frac{C_{44k}}{R_\alpha R_\beta} - \bar{\alpha}^2 \frac{C_{66k}H_\beta}{H_\alpha} - \bar{\beta}^2 \frac{C_{22k}H_\alpha}{H_\beta} + \rho_k H_\alpha H_\beta \omega^2 \right) V_k + \\ & \left( \bar{\beta} \frac{C_{44k}H_\alpha}{H_\beta R_\beta} + \bar{\beta} \frac{C_{44k}}{R_\alpha} + \bar{\beta} \frac{C_{22k}H_\alpha}{H_\beta R_\beta} + \bar{\beta} \frac{C_{12k}}{R_\alpha} \right) W_k + \left( \frac{C_{44k}H_\alpha}{R_\beta} + \frac{C_{44k}H_\beta}{R_\alpha} \right) V_{k,z} + \left( \bar{\beta}C_{44k}H_\alpha + \right. \\ & \left. \bar{\beta}C_{23k}H_\alpha \right) W_{k,z} + \left( C_{44k}H_\alpha H_\beta \right) V_{k,zz} = 0, \end{aligned} \quad (42)$$

$$\begin{aligned} & \left( \bar{\alpha} \frac{C_{55k}H_\beta}{H_\alpha R_\alpha} - \bar{\alpha} \frac{C_{13k}}{R_\beta} + \bar{\alpha} \frac{C_{11k}H_\beta}{H_\alpha R_\alpha} + \bar{\alpha} \frac{C_{12k}}{R_\beta} \right) U_k + \left( \bar{\beta} \frac{C_{44k}H_\alpha}{H_\beta R_\beta} - \bar{\beta} \frac{C_{23k}}{R_\alpha} + \bar{\beta} \frac{C_{22k}H_\alpha}{H_\beta R_\beta} + \bar{\beta} \frac{C_{12k}}{R_\alpha} \right) V_k + \\ & \left( \frac{C_{13k}}{R_\alpha R_\beta} + \frac{C_{23k}}{R_\alpha R_\beta} - \frac{C_{11k}H_\beta}{H_\alpha R_\alpha^2} - \frac{2C_{12k}}{R_\alpha R_\beta} - \frac{C_{22k}H_\alpha}{H_\beta R_\beta^2} - \bar{\alpha}^2 \frac{C_{55k}H_\beta}{H_\alpha} - \bar{\beta}^2 \frac{C_{44k}H_\alpha}{H_\beta} + \rho_k H_\alpha H_\beta \omega^2 \right) W_k + \\ & \left( -\bar{\alpha}C_{55k}H_\beta - \bar{\alpha}C_{13k}H_\beta \right) U_{k,z} + \left( -\bar{\beta}C_{44k}H_\alpha - \bar{\beta}C_{23k}H_\alpha \right) V_{k,z} + \left( \frac{C_{33k}H_\beta}{R_\alpha} + \frac{C_{33k}H_\alpha}{R_\beta} \right) W_{k,z} + \\ & \left( C_{33k}H_\alpha H_\beta \right) W_{k,zz} = 0. \end{aligned} \quad (43)$$

The system of Eqs.(41)-(43) can be written in a compact form by introducing coefficients  $A_{sk}$  for each block  $\left( \begin{smallmatrix} \phantom{0} \end{smallmatrix} \right)$  with  $s$  from 1 to 19:

$$A_{1k}U_k + A_{2k}V_k + A_{3k}W_k + A_{4k}U_{k,z} + A_{5k}W_{k,z} + A_{6k}U_{k,zz} = 0, \quad (44)$$

$$A_{7k}U_k + A_{8k}V_k + A_{9k}W_k + A_{10k}V_{k,z} + A_{11k}W_{k,z} + A_{12k}V_{k,zz} = 0, \quad (45)$$

$$A_{13k}U_k + A_{14k}V_k + A_{15k}W_k + A_{16k}U_{k,z} + A_{17k}V_{k,z} + A_{18k}W_{k,z} + A_{19k}W_{k,zz} = 0. \quad (46)$$

The Eqs.(44)-(46) are a system of three second order differential equations. They are written for spherical shell panels with constant radii of curvature but they automatically degenerate into equations for cylindrical shells and plates.

#### 4.1 Solution for the multilayered structures

The system of second order differential equations can be reduced to a system of first order differential equations by using the method described in [48] and [49]. A simple example to understand this reduction is shown in [48]:

$$a_1 u_1'' + b_1 u_1' + c_1 u_1 = f_1, \quad (47)$$

$$a_2 u_2'' + b_2 u_2' + c_2 u_2 = f_2, \quad (48)$$

where  $u_r''$  indicates  $u_{r,zz}$  and  $u_r'$  indicates  $u_{r,z}$ .  $f_1$  and  $f_2$  are the external loads that in the present free vibration analysis are zero. The following identities can be imposed:

$$a_1 u_1' = a_1 u_1', \quad (49)$$

$$a_2 u_2' = a_2 u_2', \quad (50)$$

the system of Eqs.(47)-(50) can be written as:

$$\begin{bmatrix} a_1 & 0 & 0 & 0 \\ 0 & a_1 & 0 & 0 \\ 0 & 0 & a_2 & 0 \\ 0 & 0 & 0 & a_2 \end{bmatrix} \begin{bmatrix} u_1 \\ u'_1 \\ u_2 \\ u'_2 \end{bmatrix}' = \begin{bmatrix} 0 & a_1 & 0 & 0 \\ -c_1 & -b_1 & 0 & 0 \\ 0 & 0 & 0 & a_2 \\ 0 & 0 & -c_2 & -b_2 \end{bmatrix} \begin{bmatrix} u_1 \\ u'_1 \\ u_2 \\ u'_2 \end{bmatrix} + \begin{bmatrix} 0 \\ f_1 \\ 0 \\ f_2 \end{bmatrix}. \quad (51)$$

The methodology described in Eqs.(47)-(51) can also be applied to the system of Eqs.(44)-(46):

$$\begin{bmatrix} A_{6k} & 0 & 0 & 0 & 0 & 0 \\ 0 & A_{12k} & 0 & 0 & 0 & 0 \\ 0 & 0 & A_{19k} & 0 & 0 & 0 \\ 0 & 0 & 0 & A_{6k} & 0 & 0 \\ 0 & 0 & 0 & 0 & A_{12k} & 0 \\ 0 & 0 & 0 & 0 & 0 & A_{19k} \end{bmatrix} \begin{bmatrix} U_k \\ V_k \\ W_k \\ U'_k \\ V'_k \\ W'_k \end{bmatrix}' = \begin{bmatrix} 0 & 0 & 0 & A_{6k} & 0 & 0 \\ 0 & 0 & 0 & 0 & A_{12k} & 0 \\ 0 & 0 & 0 & 0 & 0 & A_{19k} \\ -A_{1k} & -A_{2k} & -A_{3k} & -A_{4k} & 0 & -A_{5k} \\ -A_{7k} & -A_{8k} & -A_{9k} & 0 & -A_{10k} & -A_{11k} \\ -A_{13k} & -A_{14k} & -A_{15k} & -A_{16k} & -A_{17k} & -A_{18k} \end{bmatrix} \begin{bmatrix} U_k \\ V_k \\ W_k \\ U'_k \\ V'_k \\ W'_k \end{bmatrix}. \quad (52)$$

Eq.(52) can be written in a compact form for a generic  $k$  layer:

$$\mathbf{D}_k \frac{\partial \mathbf{U}_k}{\partial \tilde{z}} = \mathbf{A}_k \mathbf{U}_k, \quad (53)$$

where  $\frac{\partial \mathbf{U}_k}{\partial \tilde{z}} = \mathbf{U}'_k$  and  $\mathbf{U}_k = [U_k \ V_k \ W_k \ U'_k \ V'_k \ W'_k]$ . The Eq.(53) can be written as:

$$\mathbf{D}_k \mathbf{U}'_k = \mathbf{A}_k \mathbf{U}_k, \quad (54)$$

$$\mathbf{U}'_k = \mathbf{D}_k^{-1} \mathbf{A}_k \mathbf{U}_k, \quad (55)$$

$$\mathbf{U}'_k = \mathbf{A}_k^* \mathbf{U}_k, \quad (56)$$

with  $\mathbf{A}_k^* = \mathbf{D}_k^{-1} \mathbf{A}_k$ .

In the case of plate geometry coefficients  $A_{3k}$ ,  $A_{4k}$ ,  $A_{9k}$ ,  $A_{10k}$ ,  $A_{13k}$ ,  $A_{14k}$  and  $A_{18k}$  are zero because the radii of curvature  $R_\alpha$  and  $R_\beta$  are infinite. The other coefficients  $A_{1k}$ ,  $A_{2k}$ ,  $A_{5k}$ ,  $A_{6k}$ ,  $A_{7k}$ ,  $A_{8k}$ ,  $A_{11k}$ ,  $A_{12k}$ ,  $A_{15k}$ ,  $A_{16k}$ ,  $A_{17k}$  and  $A_{19k}$  are constant in each  $k$  layer because parametric coefficients  $H_\alpha = H_\beta = 1$  and they do not depend on the thickness coordinate  $\tilde{z}$ , therefore matrices  $\mathbf{D}_k$ ,  $\mathbf{A}_k$  and  $\mathbf{A}_k^*$  are constant in each  $k$  layer of the plate. The solution of Eq.(56) for the plate case can be written as [49], [50]:

$$\mathbf{U}_k(\tilde{z}_k) = \exp(\mathbf{A}_k^* \tilde{z}_k) \mathbf{U}_k(0) \quad \text{with} \quad \tilde{z}_k \in [0, h_k], \quad (57)$$

where  $\tilde{z}_k$  is the thickness coordinate of each layer from 0 at the bottom to  $h_k$  at the top (see Fig. 2). The exponential matrix for the plate case (constant coefficients  $A_{sk}$ ) is calculated with  $\tilde{z}_k = h_k$  for each  $k$  layer as:

$$\mathbf{A}_k^{**} = \exp(\mathbf{A}_k^* h_k) = \mathbf{I} + \mathbf{A}_k^* h_k + \frac{\mathbf{A}_k^{*2}}{2!} h_k^2 + \frac{\mathbf{A}_k^{*3}}{3!} h_k^3 + \dots + \frac{\mathbf{A}_k^{*N}}{N!} h_k^N, \quad (58)$$

where  $\mathbf{I}$  is the  $6 \times 6$  identity matrix. This expansion has a fast convergence as indicated in [51] and it is not time consuming from the computational point of view,  $N = 15$  gives the exact solution for each possible one-layered plate case [1]. In the case of  $N_L$  layers for shell geometry  $\mathbf{A}_k^*$  is not constant in each  $k$  layer because of  $H_\alpha(\tilde{z})$  and  $H_\beta(\tilde{z})$ . First of all,  $N_L - 1$  transfer matrices  $\mathbf{T}_{k-1,k}$  must be calculated by using for each interface the following conditions for interlaminar continuity of displacements and transverse shear/normal stresses:

$$u_k^b = u_{k-1}^t, \quad v_k^b = v_{k-1}^t, \quad w_k^b = w_{k-1}^t, \quad (59)$$

$$\sigma_{zzk}^b = \sigma_{zzk-1}^t, \quad \sigma_{\alpha zk}^b = \sigma_{\alpha zk-1}^t, \quad \sigma_{\beta zk}^b = \sigma_{\beta zk-1}^t, \quad (60)$$

that means each displacement and transverse stress component at the top (t) of the  $k-1$  layer is equal to displacement and transverse stress components at the bottom (b) of the  $k$  layer.

The continuity of transverse shear stress  $\sigma_{\alpha z}$  is given as:

$$\frac{C_{55k-1}}{H_{\alpha k-1}^t} \bar{\alpha} W_{k-1}^t + C_{55k-1} U_{k-1}'^t - \frac{C_{55k-1}}{H_{\alpha k-1}^t} U_{k-1}^t = \frac{C_{55k}}{H_{\alpha k}^b} \bar{\alpha} W_k^b + C_{55k} U_k'^b - \frac{C_{55k}}{H_{\alpha k}^b} U_k^b, \quad (61)$$

$$U_k'^b = \frac{1}{C_{55k}} \left( \frac{C_{55k-1}}{H_{\alpha k-1}^t} \bar{\alpha} - \frac{C_{55k}}{H_{\alpha k}^b} \bar{\alpha} \right) W_{k-1}^t + \frac{1}{C_{55k}} \left( -\frac{C_{55k-1}}{H_{\alpha k-1}^t} R_{\alpha} + \frac{C_{55k}}{H_{\alpha k}^b} R_{\alpha} \right) U_{k-1}^t + \left( \frac{C_{55k-1}}{C_{55k}} \right) U_{k-1}'^t. \quad (62)$$

The continuity of transverse shear stress  $\sigma_{\beta z}$  is given as:

$$\frac{C_{44k-1}}{H_{\beta k-1}^t} \bar{\beta} W_{k-1}^t + C_{44k-1} V_{k-1}'^t - \frac{C_{44k-1}}{H_{\beta k-1}^t} V_{k-1}^t = \frac{C_{44k}}{H_{\beta k}^b} \bar{\beta} W_k^b + C_{44k} V_k'^b - \frac{C_{44k}}{H_{\beta k}^b} V_k^b, \quad (63)$$

$$V_k'^b = \frac{1}{C_{44k}} \left( \frac{C_{44k-1}}{H_{\beta k-1}^t} \bar{\beta} - \frac{C_{44k}}{H_{\beta k}^b} \bar{\beta} \right) W_{k-1}^t + \frac{1}{C_{44k}} \left( -\frac{C_{44k-1}}{H_{\beta k-1}^t} R_{\beta} + \frac{C_{44k}}{H_{\beta k}^b} R_{\beta} \right) V_{k-1}^t + \left( \frac{C_{44k-1}}{C_{44k}} \right) V_{k-1}'^t. \quad (64)$$

The continuity of transverse normal stress  $\sigma_{zz}$  is given as:

$$\begin{aligned} & -\frac{C_{13k-1}}{H_{\alpha k-1}^t} \bar{\alpha} U_{k-1}^t + \frac{C_{13k-1}}{H_{\alpha k-1}^t} R_{\alpha} W_{k-1}^t - \frac{C_{23k-1}}{H_{\beta k-1}^t} \bar{\beta} V_{k-1}^t + \frac{C_{23k-1}}{H_{\beta k-1}^t} R_{\beta} W_{k-1}^t + C_{33k-1} W_{k-1}'^t = \\ & -\frac{C_{13k}}{H_{\alpha k}^b} \bar{\alpha} U_k^b + \frac{C_{13k}}{H_{\alpha k}^b} R_{\alpha} W_k^b - \frac{C_{23k}}{H_{\beta k}^b} \bar{\beta} V_k^b + \frac{C_{23k}}{H_{\beta k}^b} R_{\beta} W_k^b + C_{33k} W_k'^b, \end{aligned} \quad (65)$$

$$\begin{aligned} W_k'^b &= \frac{1}{C_{33k}} \left( -\frac{C_{13k-1}}{H_{\alpha k-1}^t} \bar{\alpha} + \frac{C_{13k}}{H_{\alpha k}^b} \bar{\alpha} \right) U_{k-1}^t + \frac{1}{C_{33k}} \left( -\frac{C_{23k-1}}{H_{\beta k-1}^t} \bar{\beta} + \frac{C_{23k}}{H_{\beta k}^b} \bar{\beta} \right) V_{k-1}^t + \\ & \frac{1}{C_{33k}} \left( \frac{C_{13k-1}}{H_{\alpha k-1}^t} R_{\alpha} + \frac{C_{23k-1}}{H_{\beta k-1}^t} R_{\beta} - \frac{C_{13k}}{H_{\alpha k}^b} R_{\alpha} - \frac{C_{23k}}{H_{\beta k}^b} R_{\beta} \right) W_{k-1}^t + \left( \frac{C_{33k-1}}{C_{33k}} \right) W_{k-1}'^t. \end{aligned} \quad (66)$$

The continuity of displacement components is:

$$U_k^b = U_{k-1}^t, \quad V_k^b = V_{k-1}^t, \quad W_k^b = W_{k-1}^t. \quad (67)$$

In Eqs.(61)-(67),  $t$  and  $b$  indicate top and bottom of  $k-1$  layer and  $k$  layer, respectively.  $\bar{\alpha}$ ,  $\bar{\beta}$ ,  $R_{\alpha}$  and  $R_{\beta}$  refer to mid-surface  $\Omega_0$  of the structure.  $H_{\alpha}$  and  $H_{\beta}$  are calculated at the interfaces between  $k-1$  layer and  $k$  layer. The Eqs.(61)-(67) can be grouped in a system:

$$\begin{bmatrix} U \\ V \\ W \\ U' \\ V' \\ W' \end{bmatrix}_k^b = \begin{bmatrix} 1 & 0 & 0 & 0 & 0 & 0 \\ 0 & 1 & 0 & 0 & 0 & 0 \\ 0 & 0 & 1 & 0 & 0 & 0 \\ T_1 & 0 & T_2 & T_3 & 0 & 0 \\ 0 & T_4 & T_5 & 0 & T_6 & 0 \\ T_7 & T_8 & T_9 & 0 & 0 & T_{10} \end{bmatrix}_{k-1,k} \begin{bmatrix} U \\ V \\ W \\ U' \\ V' \\ W' \end{bmatrix}_{k-1}^t, \quad (68)$$

Eq.(68) in compact form is:

$$\mathbf{U}_k^b = \mathbf{T}_{k-1,k} \mathbf{U}_{k-1}^t. \quad (69)$$

The calculated  $\mathbf{T}_{k-1,k}$  matrices allow to link  $\mathbf{U}$  at the bottom (b) of the  $k$  layer with  $\mathbf{U}$  at the top (t) of the  $k-1$  layer. Eq.(69) can also be written as:

$$\mathbf{U}_k(0) = \mathbf{T}_{k-1,k} \mathbf{U}_{k-1}(h_{k-1}), \quad (70)$$

where  $\mathbf{U}_k$  is calculated for  $\tilde{z}_k = 0$  and  $\mathbf{U}_{k-1}$  is calculated for  $\tilde{z}_{k-1} = h_{k-1}$ .  $\mathbf{U}$  at the top of the  $k$  layer is linked with  $\mathbf{U}$  at the bottom of the same  $k$  layer by means of the exponential matrix  $\mathbf{A}_k^{**}$ :

$$\mathbf{U}_k(h_k) = \mathbf{A}_k^{**} \mathbf{U}_k(0), \quad (71)$$

Eq.(70) can recursively be introduced in Eq.(71) for the  $N_L - 1$  interfaces to obtain:

$$\mathbf{U}_{N_L}(h_{N_L}) = \mathbf{A}_{N_L}^{**} \mathbf{T}_{N_L-1, N_L} \mathbf{A}_{N_L-1}^{**} \mathbf{T}_{N_L-2, N_L-1} \dots \mathbf{A}_2^{**} \mathbf{T}_{1,2} \mathbf{A}_1^{**} \mathbf{U}_1(0), \quad (72)$$

the definition of the matrix  $\mathbf{H}_m$  for the multilayered plate allows Eq.(72) to be written as:

$$\mathbf{U}_{N_L}(h_{N_L}) = \mathbf{H}_m \mathbf{U}_1(0), \quad (73)$$

that links  $\mathbf{U}$  calculated at the top of the last  $N_L$  layer with  $\mathbf{U}$  calculated at the bottom of the first layer. In the case of multilayered plates matrices  $\mathbf{D}_k$ ,  $\mathbf{A}_k$  and  $\mathbf{A}_k^*$  are constant in each  $k$  layer because  $R_\alpha$  and  $R_\beta$  are infinite and  $H_\alpha$  and  $H_\beta$  equal 1. In the case of shell geometry matrices  $\mathbf{D}_k$ ,  $\mathbf{A}_k$  and  $\mathbf{A}_k^*$  are not constant in each layer because of parametric coefficients  $H_\alpha$  and  $H_\beta$  that depend on  $\tilde{z}$  coordinate (see Fig. 2). A first method could be the use of hypothesis  $\frac{z}{R_\alpha} = \frac{z}{R_\beta} = 0$  (it is valid only for very thin shells) that means  $H_\alpha = H_\beta = 1$ . In this case the solution is the same already seen for the plate because matrices  $\mathbf{D}_k$ ,  $\mathbf{A}_k$  and  $\mathbf{A}_k^*$  are constant in each  $k$  layer. This method is not used in this paper because it is an approximation that is valid only for very thin shells, and it does not consider the exact geometry of the structure. The second method (used in this paper) is the introduction of several  $j$  fictitious layers in each  $k$  layer where  $H_\alpha$  and  $H_\beta$  can exactly be calculated. Matrices  $\mathbf{A}_j^{**}$  are constant in the  $j$  layer because they are evaluated with  $R_\alpha$ ,  $R_\beta$ ,  $\bar{\alpha}$  and  $\bar{\beta}$  calculated in the mid-surface  $\Omega_0$  of the whole shell, and with  $H_\alpha$  and  $H_\beta$  calculated in the middle of each  $j$  layer. Matrices  $\mathbf{T}_{j-1,j}$  are also constant because they are evaluated with  $R_\alpha$ ,  $R_\beta$ ,  $\bar{\alpha}$  and  $\bar{\beta}$  calculated in the mid-surface  $\Omega_0$  of the shell, and with  $H_\alpha$  and  $H_\beta$  calculated at each fictitious interface. In the present paper each  $k$  layer of the multilayered shell is divided in  $j=M=10$  fictitious layers where we can recursively apply the Eqs.(61)-(72) with index  $q$  in place of index  $k$ . The thickness of each layer is  $h_q$ . The index  $q$  considers all the fictitious and physical layers and it goes from 1 to  $P$ .  $M = 15$  for each skin layer and  $M = 70$  for each core layer with  $N = 3$  for the exponential matrix in Eq.(58) guarantee the exact convergence for each shell investigated. The total number of mathematical layers for a multilayered shell is  $P = 100$ .

The structures are simply supported and free stresses at the top and at the bottom of the whole multilayered shell, this feature means:

$$\sigma_{zz} = \sigma_{\alpha z} = \sigma_{\beta z} = 0 \quad \text{for} \quad z = -h/2, +h/2 \quad \text{or} \quad \tilde{z} = 0, h, \quad (74)$$

$$w = v = 0, \sigma_{\alpha\alpha} = 0 \quad \text{for} \quad \alpha = 0, a, \quad (75)$$

$$w = u = 0, \sigma_{\beta\beta} = 0 \quad \text{for} \quad \beta = 0, b, \quad (76)$$

Transverse shear/normal stresses written for a generic value of  $\tilde{z}$  in the  $q$  layer are:

$$\begin{aligned} \sigma_{zzq}(\tilde{z}) = & \frac{C_{13q}}{H_\alpha(\tilde{z})} u_{q,\alpha} + \frac{C_{13q}}{H_\alpha(\tilde{z})R_\alpha} w_q + \frac{C_{23q}}{H_\beta(\tilde{z})} v_{q,\beta} + \frac{C_{23q}}{H_\beta(\tilde{z})R_\beta} w_q + C_{33q} w_{q,z} = -\bar{\alpha} \frac{C_{13q}}{H_\alpha(\tilde{z})} U_q + \\ & \frac{C_{13q}}{H_\alpha(\tilde{z})R_\alpha} W_q - \bar{\beta} \frac{C_{23q}}{H_\beta(\tilde{z})} V_q + \frac{C_{23q}}{H_\beta(\tilde{z})R_\beta} W_q + C_{33q} W_{q,z}, \end{aligned} \quad (77)$$

$$\sigma_{\beta zq}(\tilde{z}) = \frac{C_{44q}}{H_\beta(\tilde{z})} w_{q,\beta} + C_{44q} v_{q,z} - \frac{C_{44q}}{H_\beta(\tilde{z})R_\beta} v_q = \bar{\beta} \frac{C_{44q}}{H_\beta(\tilde{z})} W_q + C_{44q} V_{q,z} - \frac{C_{44q}}{H_\beta(\tilde{z})R_\beta} V_q, \quad (78)$$

$$\sigma_{\alpha zq}(\tilde{z}) = \frac{C_{55q}}{H_\alpha(\tilde{z})} w_{q,\alpha} + C_{55q} u_{q,z} - \frac{C_{55q}}{H_\alpha(\tilde{z})R_\alpha} u_q = \bar{\alpha} \frac{C_{55q}}{H_\alpha(\tilde{z})} W_q + C_{55q} U_{q,z} - \frac{C_{55q}}{H_\alpha(\tilde{z})R_\alpha} U_q, \quad (79)$$

Eq.(74) imposed at the the top (t) of the last  $P$  layer uses Eqs.(77)-(79) with  $R_\alpha$ ,  $R_\beta$ ,  $\bar{\alpha}$  and  $\bar{\beta}$  calculated in the mid-surface  $\Omega_0$  of the shell, and with  $H_\alpha^t$  and  $H_\beta^t$  calculated at top of the whole shell for  $\tilde{z} = h$ :

$$\sigma_{zzP}^t = -\bar{\alpha} \frac{C_{13P}}{H_\alpha^t} U_P^t + \frac{C_{13P}}{H_\alpha^t R_\alpha} W_P^t - \bar{\beta} \frac{C_{23P}}{H_\beta^t} V_P^t + \frac{C_{23P}}{H_\beta^t R_\beta} W_P^t + C_{33P} W_{P,z}^t = 0, \quad (80)$$

$$\sigma_{\beta zP}^t = \bar{\beta} \frac{C_{44P}}{H_\beta^t} W_P^t + C_{44P} V_{P,z}^t - \frac{C_{44P}}{H_\beta^t R_\beta} V_P^t = 0, \quad (81)$$

$$\sigma_{\alpha zP}^t = \bar{\alpha} \frac{C_{55P}}{H_\alpha^t} W_P^t + C_{55P} U_{P,z}^t - \frac{C_{55P}}{H_\alpha^t R_\alpha} U_P^t = 0, \quad (82)$$

Eq.(74) imposed at the the bottom (b) of the first layer ( $q = 1$ ) uses Eqs.(77)-(79) with  $R_\alpha$ ,  $R_\beta$ ,  $\bar{\alpha}$  and  $\bar{\beta}$  calculated in the mid-surface  $\Omega_0$  of the shell, and with  $H_\alpha^b$  and  $H_\beta^b$  calculated at bottom of the whole shell for  $\tilde{z} = 0$ :

$$\sigma_{zz1}^b = -\bar{\alpha} \frac{C_{131}}{H_\alpha^b} U_1^b + \frac{C_{131}}{H_\alpha^b R_\alpha} W_1^b - \bar{\beta} \frac{C_{231}}{H_\beta^b} V_1^b + \frac{C_{231}}{H_\beta^b R_\beta} W_1^b + C_{331} W_{1,z}^b = 0, \quad (83)$$

$$\sigma_{\beta z1}^b = \bar{\beta} \frac{C_{441}}{H_\beta^b} W_1^b + C_{441} V_{1,z}^b - \frac{C_{441}}{H_\beta^b R_\beta} V_1^b = 0, \quad (84)$$

$$\sigma_{\alpha z1}^b = \bar{\alpha} \frac{C_{551}}{H_\alpha^b} W_1^b + C_{551} U_{1,z}^b - \frac{C_{551}}{H_\alpha^b R_\alpha} U_1^b = 0. \quad (85)$$

Eqs.(80)-(82) in matrix form are ( $U_P(h_P)$  means  $U$  calculated at the top of the whole multilayered shell, last  $P$  layer with  $\tilde{z}_P = h_P$ ):

$$\begin{bmatrix} -\bar{\alpha} \frac{C_{13P}}{H_\alpha^t} & -\bar{\beta} \frac{C_{23P}}{H_\beta^t} & (\frac{C_{13P}}{H_\alpha^t R_\alpha} + \frac{C_{23P}}{H_\beta^t R_\beta}) & 0 & 0 & C_{33P} \\ 0 & -\frac{C_{44P}}{H_\beta^t R_\beta} & \bar{\beta} \frac{C_{44P}}{H_\beta^t} & 0 & C_{44P} & 0 \\ -\frac{C_{55P}}{H_\alpha^t R_\alpha} & 0 & \bar{\alpha} \frac{C_{55P}}{H_\alpha^t} & C_{55P} & 0 & 0 \end{bmatrix} \begin{bmatrix} U_P(h_P) \\ V_P(h_P) \\ W_P(h_P) \\ U_P'(h_P) \\ V_P'(h_P) \\ W_P'(h_P) \end{bmatrix} = \begin{bmatrix} 0 \\ 0 \\ 0 \end{bmatrix}. \quad (86)$$

Eqs.(83)-(85) in matrix form are ( $U_1(0)$  means  $U$  calculated at the bottom of the whole multilayered shell, first layer 1 with  $\tilde{z}_1 = 0$ ):

$$\begin{bmatrix} -\bar{\alpha} \frac{C_{131}}{H_\alpha^b} & -\bar{\beta} \frac{C_{231}}{H_\beta^b} & (\frac{C_{131}}{H_\alpha^b R_\alpha} + \frac{C_{231}}{H_\beta^b R_\beta}) & 0 & 0 & C_{331} \\ 0 & -\frac{C_{441}}{H_\beta^b R_\beta} & \bar{\beta} \frac{C_{441}}{H_\beta^b} & 0 & C_{441} & 0 \\ -\frac{C_{551}}{H_\alpha^b R_\alpha} & 0 & \bar{\alpha} \frac{C_{551}}{H_\alpha^b} & C_{551} & 0 & 0 \end{bmatrix} \begin{bmatrix} U_1(0) \\ V_1(0) \\ W_1(0) \\ U_1'(0) \\ V_1'(0) \\ W_1'(0) \end{bmatrix} = \begin{bmatrix} 0 \\ 0 \\ 0 \end{bmatrix}. \quad (87)$$

Eqs.(86) and (87) in compact form to express the free stress state at the top and bottom of the whole shell are:

$$B_P(h_P) U_P(h_P) = 0, \quad (88)$$

$$B_1(0) U_1(0) = 0, \quad (89)$$

Eq.(73) can be substituted in Eq.(88) considering a total number of layers equals  $P$ :

$$B_P(h_P) H_m U_1(0) = 0, \quad (90)$$

$$B_1(0) U_1(0) = 0, \quad (91)$$

in this way Eqs.(90) and (91) are grouped in the following system:

$$\begin{bmatrix} \mathbf{B}_P(h_P) & \mathbf{H}_m \\ \mathbf{B}_1(0) & \end{bmatrix} \begin{bmatrix} \mathbf{U}_1(0) \end{bmatrix} = \begin{bmatrix} 0 \end{bmatrix}, \quad (92)$$

and introducing the  $(6 \times 6)$   $\mathbf{E}$  matrix, the Eq.(92) is:

$$\begin{bmatrix} \mathbf{E} \end{bmatrix} \begin{bmatrix} \mathbf{U}_1(0) \end{bmatrix} = \begin{bmatrix} 0 \end{bmatrix}. \quad (93)$$

The Eq.(93) is also valid for plate case where the fictitious layers are not introduced and  $\mathbf{B}_{N_L}(h_{N_L}) = \mathbf{B}_P(h_P)$ . Matrix  $\mathbf{E}$  has always  $(6 \times 6)$  dimension, independently from number of layers  $P$ , even if the method uses a layer-wise approach. The solution is implemented in a Matlab code where only the spherical shell method is considered, it automatically degenerates into cylindrical open/closed shell and plate methods.

The free vibration analysis means to find the non-trivial solution of  $\mathbf{U}_1(0)$  in Eq.(93), this means to impose the determinant of matrix  $\mathbf{E}$  equals zero:

$$\det[\mathbf{E}] = 0, \quad (94)$$

Eq.(94) means to find the roots of an higher order polynomial in  $\lambda = \omega^2$ . For each pair of half-wave numbers  $(m, n)$  a certain number of circular frequencies are obtained depending on the order  $N$  chosen for each exponential matrix  $\mathbf{A}_q^{**}$ .

## 4.2 Vibration modes

A certain number of circular frequencies  $\omega_l$  are found when half-wave numbers  $m$  and  $n$  are imposed in the structures. For each frequency  $\omega_l$ , it is possible to find the vibration mode through the thickness in terms of the three displacement components. If the frequency  $\omega_l$  is substituted in  $(6 \times 6)$  matrix  $\mathbf{E}$ , this last matrix has six eigenvalues. We are interested to the null space of matrix  $\mathbf{E}$  that means to find the  $(6 \times 1)$  eigenvector related to the minimum of the six eigenvalues proposed. This null space is, for the chosen frequency  $\omega_l$ , the vector  $\mathbf{U}$  calculated at the bottom of the whole structure:

$$\mathbf{U}_{1\omega_l}(0) = \begin{bmatrix} U_1(0) & V_1(0) & W_1(0) & U'_1(0) & V'_1(0) & W'_1(0) \end{bmatrix}_{\omega_l}^T, \quad (95)$$

$T$  means the transpose of the vector and the subscript  $\omega_l$  means that the null space is calculated for the circular frequency  $\omega_l$ .

It is possible to find  $\mathbf{U}_{q\omega_l}(\tilde{z}_q)$  (with the three displacement components  $U_{q\omega_l}(\tilde{z}_q)$ ,  $V_{q\omega_l}(\tilde{z}_q)$  and  $W_{q\omega_l}(\tilde{z}_q)$  through the thickness) for each  $q$  layer of the multilayered structure by using Eqs.(70)-(73) with the index  $q$  from 1 to  $P$ . The thickness coordinate  $\tilde{z}$  can assume all the values from the bottom to the top of the structure. For the plate case the procedure is simpler because there are not the  $j$  fictitious layers and the index  $q$  coincides with the index  $k$  of the physical layers (in this case, total number of layers is  $N_L$ ).

## 5 Results

The present three-dimensional exact solution proposed for the free vibration analysis of multilayered plates and shells has been validated by means of a comparison with assessments given in the literature. These assessments are the free vibration analysis of multilayered composite square plates proposed in [10], and cylindrical and spherical shell panel free vibration analysis shown in [29]. After this preliminary validation the method can be used with confidence to investigate the free vibrations of multilayered sandwich square and rectangular plates, cylindrical shell panels, cylinders and spherical shell panels (see Fig. 3). In the assessments and benchmarks proposed the 3D solution is always obtained with a total number  $M=100$  of mathematical layers and an expansion order  $N=3$  for the exponential matrix.

## 5.1 Validation of the method

The assessment proposed by Messina [10] considers a simply supported square plate ( $a=b=10$ ) with thickness ratio  $a/h=10$ . The plate is multilayered and each composite layer has Young modulus components  $E_1 = 25.1 \times 10^6 \text{ psi}$ ,  $E_2 = 4.8 \times 10^6 \text{ psi}$  and  $E_3 = 0.75 \times 10^6 \text{ psi}$ , shear modulus components  $G_{12} = 1.36 \times 10^6 \text{ psi}$ ,  $G_{13} = 1.2 \times 10^6 \text{ psi}$  and  $G_{23} = 0.47 \times 10^6 \text{ psi}$ , Poisson ratio components  $\nu_{12} = 0.036$ ,  $\nu_{13} = 0.25$  and  $\nu_{23} = 0.171$ . The mass density is  $\rho = 0.054191 \text{ lb/in}^3$ . The first three vibration modes are given in Table 1 in terms of no-dimensional circular frequency  $\bar{\omega} = \omega h \sqrt{\rho/E_2}$  for half-wave numbers (m,n) equal (1,1), (1,2), (2,1) and (2,2). Two-layered, three-layered and four-layered composite plates are investigated with lamination sequence  $(0^\circ/90^\circ)$ ,  $(0^\circ/90^\circ/0^\circ)$  and  $(0^\circ/90^\circ/0^\circ/90^\circ)$ , respectively (each layer has the same thickness). The present three-dimensional solution coincides with that given by Messina [10] for each half-wave number imposed, lamination sequence and mode considered. This validation is fundamental because the present three-dimensional solution extended to general orthogonal curvilinear coordinates uses a methodology similar to the one applied by Messina [10] to plates with orthogonal rectilinear coordinates.

The assessment proposed in Table 2 considers a simply supported cylindrical shell panel with radius of curvature  $R_\alpha = 10$  and thickness  $h = 0.5$ . The radius of curvature in  $\beta$  direction is infinite and the shell has dimensions  $a = b = 5$ . The structure is multilayered (it embeds  $N_L$  layers) and each layer has the same thickness. The lamination sequence is  $(0^\circ/90^\circ/0^\circ/90^\circ/\dots)$ . Table 2 gives the first three modes for imposed half-wave numbers (1,1) and the first mode for the other imposed half-wave numbers (m,n). The results are given as no-dimensional circular frequency  $\bar{\omega} = \omega R_\beta \sqrt{\rho/E_0}$  for number of layers  $N_L$  equals 2, 4 and 10. Each composite layer has Young modulus components  $E_1 = 25E_0$  and  $E_2 = E_3 = E_0$ , shear modulus components  $G_{12} = G_{13} = 0.5E_0$  and  $G_{23} = 0.2E_0$ , Poisson ratio components  $\nu_{12} = \nu_{13} = \nu_{23} = 0.25$ . The mass density is  $\rho = 1500 \text{ kg/m}^3$ . The three-dimensional solution proposed by Huang [29] is coincident with the present three-dimensional analysis for each half-wave number imposed, number of layers ( $N_L$ ) and mode considered. The two solutions give the same results even if the two methods use different approaches.

The assessment proposed in Table 3 considers a simply supported spherical shell panel with radii of curvature  $R_\alpha = R_\beta = 10$ , thickness  $h = 0.2$  and dimensions  $a = b = 2$ . The structure is multilayered (it embeds  $N_L$  layers) and each layer has the same thickness. The lamination sequence is  $(0^\circ/90^\circ/0^\circ/90^\circ/\dots)$ . Table 3 gives the first fundamental mode for different half-wave numbers (m,n) imposed. The results are given as circular frequencies with the same no-dimensional form already seen for the assessment of Table 2. The spherical shell panel embeds the same composite material of the cylindrical shell panel. The three-dimensional solution proposed by Huang [29] is coincident with the present three-dimensional analysis for each pair of half-wave numbers (m,n) imposed and number of layers ( $N_L$ ) considered.

After these three preliminary assessments, the present three-dimensional solution can be considered as validated for the free vibration analysis of multilayered plates and shells.

## 5.2 Benchmarks

Five different geometries are analyzed as shown in Fig. 3. The square plate has dimensions  $a = b = 1$  and thickness ratios  $a/h = 100, 50, 10, 5$ . The rectangular plate has dimensions  $a = 1$  and  $b = 3a$  and the thickness ratios are  $a/h = 100, 50, 10, 5$ . The cylindrical shell panel has a radius of curvature  $R_\alpha = 10$  and an infinite radius of curvature  $R_\beta$  in  $\beta$  direction. The dimensions are  $a = \frac{\pi}{3} R_\alpha$  and  $b = 20$ , and the thickness ratios are  $R_\alpha/h = 1000, 100, 10, 5$ . The cylinder has the same radii of curvature of the cylindrical shell panel, but it is closed in circumferential direction that means  $a = 2\pi R_\alpha$ . The other dimension is  $b = 100$  and the thickness ratios are  $R_\alpha/h = 1000, 100, 10, 5$ . The last geometry is the spherical shell panel with radii of curvature  $R_\alpha = R_\beta = 10$ , dimensions  $a = b = \frac{\pi}{3} R_\alpha$ , and thickness ratios  $R_\alpha/h = 1000, 100, 10, 5$ . All these structures are simply supported. Each geometry includes two

different sandwich configurations. The sandwich structure with isotropic skins has a foam core in PVC with thickness  $h_c = 0.7h$  (where  $h_c$  is the thickness of the core and  $h$  is the total thickness) and two external skins in isotropic aluminium alloy Al2024 with thickness  $h_s = 0.15h$  (where  $h_s$  indicates the thickness of each skin). The sandwich structure with multilayered composite faces has a foam core in PVC with thickness  $h_c = 0.7h$ , each external skin is made of two composite layers with lamination sequence  $(0^\circ/90^\circ)$  and thickness  $h_l = 0.075h$  (where  $h_l$  is the thickness of each composite layer that means  $h_s = 0.15h$  for each skin). Further details about the two sandwich configurations are given in Fig. 3. The PVC material used as foam core has Young modulus  $E = 180 \text{ MPa}$ , Poisson ratio  $\nu = 0.37$  and mass density  $\rho = 50 \text{ kg/m}^3$ . The isotropic aluminium alloy Al2024 used as skins has Young modulus  $E = 73 \text{ GPa}$ , Poisson ratio  $\nu = 0.3$  and mass density  $\rho = 2800 \text{ kg/m}^3$ . The orthotropic layers in Gr/Ep used to build the composite skins have Young modulus components  $E_1 = 132.38 \text{ GPa}$  and  $E_2 = E_3 = 10.756 \text{ GPa}$ , shear modulus components  $G_{12} = G_{13} = 5.6537 \text{ GPa}$  and  $G_{23} = 3.603 \text{ GPa}$ , Poisson ratio components  $\nu_{12} = \nu_{13} = 0.24$  and  $\nu_{23} = 0.49$ , the mass density is  $\rho = 1600 \text{ kg/m}^3$ . Ten different benchmarks are proposed to show a complete overview of the free vibration analysis of multilayered composite and sandwich plates and shells: sandwich square plate with isotropic faces (see Table 4), sandwich square plate with composite faces (see Table 5), sandwich rectangular plate with isotropic faces (see Table 6), sandwich rectangular plate with composite faces (see Table 7), sandwich cylindrical shell panel with isotropic faces (see Table 8), sandwich cylindrical shell panel with composite faces (see Table 9), sandwich cylinder with isotropic faces (see Table 10), sandwich cylinder with composite faces (see Table 11), sandwich spherical shell panel with isotropic faces (see Table 12), sandwich spherical shell panel with composite faces (see Table 13). The first three circular frequencies in no-dimensional form  $\bar{\omega} = \omega \frac{a^2}{h} \sqrt{\frac{\rho_{skin}}{E_{2skin}}}$  are calculated in Tables 4-13 for various pairs of half-wave numbers (m,n) and several thickness ratios. The vibration modes plotted in Figs. 4-8 are given in terms of no-dimensional values such as  $u^* = u/|u_{max}|$ ,  $v^* = v/|v_{max}|$ ,  $w^* = w/|w_{max}|$  and  $z^* = \tilde{z}/h$ . Circular frequencies plotted in Figs. 9-13 with respect to half-wave numbers (m,n) and vibration mode order have the same no-dimensional form already seen in the Tables 4-13.

Table 4 presents thick and thin square sandwich plates with isotropic faces (Benchmark 1). The first three vibration modes are shown for some combinations of half-wave numbers (m,n) and different thickness ratios. The plate is square and the three layers (the core and the two external faces) are isotropic. Therefore, circular frequencies for half-wave numbers (0,1) are equal to those for (1,0), and the same considerations are made for the half-wave numbers (1,2) and (2,1). Fig. 9 shows (for the case of a thick plate with isotropic faces,  $a/h = 10$ ) how the first six vibration modes change with the imposed half-wave numbers (m,n). Each vibration mode increases when the half-wave numbers increase. The (0,1) cases are equal to the (1,0) cases, and the (1,2) cases are equal to the (2,1) cases. The lowest frequency is obtained for the first mode in the case of (0,1) and (1,0) half-wave numbers. Higher order modes (third, forth, fifth and sixth ones) rapidly increase when the half-wave numbers (m,n) increase. Table 5 shows thick and thin square sandwich plates with external faces made of two composite layers (Benchmark 2). It presents the first three vibration modes for some possible combinations of half-wave numbers (m,n) from (0,1) until to (2,2). The core is made of an isotropic material, but the skins are made of composite orthotropic layers with fiber orientation  $0^\circ/90^\circ$  at the bottom and  $90^\circ/0^\circ$  at the top. For this reason, results for half-wave numbers (0,1) are not equal to those for (1,0), and the same considerations apply to the half-wave numbers (1,2) and (2,1). This feature is due to the in-plane orthotropy of the skins. Fig. 4 shows the first three vibration modes in terms of no-dimensional displacements  $u^*$ ,  $v^*$  and  $w^*$  through the no-dimensional thickness coordinate  $z^*$  for sandwich plate with composite skins and thickness ratio  $a/h = 10$  and for half-wave numbers (1,0), (1,1), (2,1) and (2,2). The first mode always has a constant through-the-thickness transverse displacement  $w^*$ , and linear in-plane displacements  $u^*$  and  $v^*$  with the typical zigzag form of the sandwich structures. This zigzag form is due to the fact that the core has completely different elastic and mass properties from those of the skins. In the case of half-wave numbers (1,0) the in-plane displacements  $v^*$  is zero. The



second mode has a linear zigzag form of the transverse displacement  $w^*$ , and a non-linear zigzag form of the in-plane displacements  $u^*$  and  $v^*$ . In the case of half-wave numbers (1,0) the only displacement different from zero is the constant value of  $v^*$ . Similar considerations can be made for the third mode, but in this case the displacement  $v^*$  has a linear zigzag form through the thickness for the (1,0) case. The typical zigzag form of displacements for sandwich structures due to the transverse anisotropy (layers with different elastic and mass properties) is shown by the present three-dimensional model because it uses a layer-wise approach for each layer embedded in the multilayered structure.

Tables 6 and 7 show the same cases already seen in Tables 4 and 5, but a rectangular plate is analyzed in place of a square plate. In Table 6 (Benchmark 3), the frequencies for (0,1) are different from those for (1,0) (same considerations can be made for (1,2) and (2,1) cases) even if the faces are isotropic because the plate is rectangular with dimension  $b = 3a$ . These features are also valid for Table 7 (Benchmark 4) where the plate is rectangular with orthotropic composite faces. Fig. 10 shows (for the case of a thick rectangular plate with isotropic faces,  $a/h = 10$ ) as the first six vibration modes change with the imposed half-wave numbers (m,n). All the considerations already made for Benchmark 1 in Fig. 9 are valid for Benchmark 3 in Fig. 10. Moreover, (0,1) cases are different from (1,0) cases, and (1,2) cases are different from (2,1) cases because the plate is rectangular. The lowest frequency is obtained for the first mode in the (0,1) case, the (1,0) case gives a higher first frequency. Fig. 5 shows the first three vibration modes for sandwich plate with composite faces and thickness ratio  $a/h = 10$  and for half-wave numbers (1,0), (1,1), (2,1) and (2,2). Benchmark 4 for the rectangular plate has vibration modes similar to those proposed in Fig. 4 for the square plate of Benchmark 2. The zigzag form of the displacements through the thickness (linear and non-linear) is confirmed because the sandwich structure has an important transverse anisotropy value between core and skins.

Table 8 gives the first three vibration modes of the sandwich cylindrical shell panel with isotropic faces (Benchmark 5) for several combinations of half-wave numbers (m,n) and different thickness ratios. The shell is isotropic but the frequencies are always different for each couple of (m,n) because of the geometry with different a and b dimensions. Similar considerations are also valid for Benchmark 6 in Table 9 (sandwich cylindrical shell panel with composite faces). The geometry with different a and b dimensions and orthotropic composite faces do not give any similarity when the half-wave numbers (m,n) change. Fig. 11 shows the first six vibration modes versus the imposed half-wave numbers (m,n) for the case of sandwich cylindrical shell panel with isotropic faces (Benchmark 5). The particular geometry of the cylindrical shell (dimensions a and b are different, and radius of curvature in  $\alpha$  direction) do not allow the lowest frequency to be identified as the first vibration mode for half-wave numbers (0,1). The lowest frequency is obtained for the first vibration mode in the (1,0) case. All the first vibration modes for higher values of half-wave numbers are smaller than the first vibration mode for (0,1), this feature is due to the coupling generated by the radius of curvature  $R_\alpha$ . Fig. 6 shows the first three vibration modes for thickness ratio  $R_\alpha/h = 10$  and composite skins, half-wave numbers are (1,0), (1,1), (2,1) and (2,2). The vibration modes have the typical zigzag form of the displacements because the shell has a sandwich structure. These vibration modes have a different behavior with respect to the behavior of plates given in Figs. 4 and 5. This difference is due to the curvature.

Tables 10 and 11 show frequencies for sandwich closed cylinders with isotropic faces (Benchmark 7) and composite faces (Benchmark 8), respectively. These results do not add further considerations with respect to those already given for the open cylindrical shell. The half-wave number m in  $\alpha$  direction must be zero or equal to even values because the structure is closed in this direction. Fig. 12 shows the first six vibration modes versus the imposed half-wave numbers (m,n) for the case of sandwich closed cylinder with isotropic faces (Benchmark 7). The particular geometry of the cylinder (dimensions a and b have different values, and  $\alpha$  direction is closed) makes it possible to identify the first mode for half-wave numbers (2,1) as lowest frequency. The first mode for (0,1) is the second lowest frequency. Important differences (in terms of vibration modes through the thickness) are shown in Fig. 7 for the sandwich cylinder with composite faces (Benchmark 8) with respect to the open cylindrical panel in

Fig. 6. In any case, the sandwich structure shows the typical zigzag form of the displacements that can be linear, constant or zero.

Tables 12 and 13 investigate sandwich spherical shell panel with isotropic faces (Benchmark 9) and orthotropic composite faces (Benchmark 10), respectively. The shell geometry considered here has the same radii of curvature in  $\alpha$  and  $\beta$  directions, and the same dimensions  $a$  and  $b$ . For this reason the considerations made for the square plate (Tables 4 and 5) are also valid in these two last benchmarks: frequencies for (0,1) and (1,0) are the same for the case with isotropic faces. This feature remains valid for half-wave numbers (1,2) and (2,1). In the cases of composite faces (Benchmark 10) the frequencies for (0,1) should be different from those for (1,0), and the frequencies for (1,2) should be different from those for (2,1). In Table 13 these differences are clear for thick shells where the physical quantity of orthotropic composite material is bigger. Fig. 13 shows (for the case of thick sandwich panel with isotropic faces,  $R_\alpha/h = 10$ ) as the first six vibration modes change with the imposed half-wave numbers (m,n). Each vibration mode increases when the half-wave numbers increase, the (0,1) cases are equal to the (1,0) cases, and the (1,2) cases are equal to the (2,1) cases. The lowest frequency is obtained for the first mode in the (0,1) and (1,0) cases. Higher order modes (third, forth, fifth and sixth ones) rapidly increase when the half-wave numbers (m,n) increase. In any case, the radii of curvature have a fundamental role in the vibration mode analysis shown in Fig. 8 for the case of sandwich configuration with orthotropic composite faces. These vibration modes are rather complicated because of the coupling generated by the radii of curvature. The displacements have the typical zigzag form caused by the difference between core and skins in terms of elastic and mass properties.

## 6 Conclusions

The general three-dimensional formulation proposed uses an exact geometry for shells and a layer-wise approach for the multilayered structures. This method allows results for spherical, open cylindrical, closed cylindrical and flat panels to be obtained. The differential equations of equilibrium in orthogonal curvilinear coordinates for the free vibrations of simply supported multilayered composite and sandwich plates and shells have been exactly solved in three-dimensional form. The first three vibration modes have been investigated for several geometries, sandwich configurations with isotropic or composite faces, various thickness ratios and half-wave numbers imposed. The vibration modes through the thickness make it possible to recognize the most complicated cases and these results will be useful benchmarks to validate future refined 2D models for the analysis of multilayered structures. The layer-wise approach proposed is obtained by imposing the continuity of displacements and transverse shear/normal stresses at the interfaces between the layers of the plates and shells. This approach allows zigzag form of displacements to be shown. This form is typical of multilayered structures with high values of transverse anisotropy. This exact solution gives a global three-dimensional overview of the free vibration problem of multilayered plates and shells.

## References

- [1] S. Brischetto, Three-dimensional exact free vibration analysis of spherical, cylindrical and flat one-layered panels, *Shock and Vibration*, 2014, 1-29, 2014.
- [2] N.J. Pagano, Exact solutions for rectangular bidirectional composites and sandwich plates, *Journal of Composite Materials*, 4, 20-34, 1970.
- [3] H.-R. Meyer-Piening, Application of the elasticity solution to linear sandwich beam, plate and shell analyses, *Journal of Sandwich Structures and Materials*, 6, 295-312, 2004.

- [4] S. Aimmanee and R.C. Batra, Analytical solution for vibration of an incompressible isotropic linear elastic rectangular plate, and frequencies missed in previous solutions, *Journal of Sound and Vibration*, 302, 613-620, 2007.
- [5] R.C. Batra and S. Aimmanee, Letter to the Editor: Missing frequencies in previous exact solutions of free vibrations of simply supported rectangular plates, *Journal of Sound and Vibration*, 265, 887-896, 2003.
- [6] S. Srinivas, C.V. Joga Rao and A.K. Rao, An exact analysis for vibration of simply-supported homogeneous and laminated thick rectangular plates, *Journal of Sound and Vibration*, 12, 187-199, 1970.
- [7] S. Srinivas, A.K. Rao and C.V.J. Rao, Flexure of simply supported thick homogeneous and laminated rectangular plates, *Zeitschrift für Angewandte Mathematik und Mechanik*, 49, 449-458, 1969.
- [8] R.C. Batra, S. Vidoli and F. Vestroni, Plane wave solutions and modal analysis in higher order shear and normal deformable plate theories, *Journal of Sound and Vibration*, 257, 63-88, 2002.
- [9] J.Q. Ye, A three-dimensional free vibration analysis of cross-ply laminated rectangular plates with clamped edges, *Computer Methods in Applied Mechanics and Engineering*, 140, 383-392, 1997.
- [10] A. Messina, Three dimensional free vibration analysis of cross-ply laminated plates through 2D and exact models, *3rd International Conference on Integrity, Reliability and Failure*, Porto (Portugal), 20-24 July 2009.
- [11] Y.K. Cheung and D. Zhou, Three-dimensional vibration analysis of cantilevered and completely free isosceles triangular plates, *International Journal of Solids and Structures*, 39, 673-687, 2002.
- [12] K.M. Liew and B. Yang, Three-dimensional elasticity solutions for free vibrations of circular plates: a polynomials-Ritz analysis, *Computer Methods in Applied Mechanics and Engineering*, 175, 189-201, 1999.
- [13] Y.B. Zhao, G.W. Wei and Y. Xiang, Discrete singular convolution for the prediction of high frequency vibration of plates, *International Journal of Solids and Structures*, 39, 65-88, 2002.
- [14] G.W. Wei, Y.B. Zhao and Y. Xiang, A novel approach for the analysis of high-frequency vibrations, *Journal of Sound and Vibration*, 257, 207-246, 2002.
- [15] H. Rokni Damavandi Taher, M. Omid, A.A. Zadpoor and A.A. Nikooyan, Short Communication: Free vibration of circular and annular plates with variable thickness and different combinations of boundary conditions, *Journal of Sound and Vibration*, 296, 1084-1092, 2006.
- [16] Y. Xing and B. Liu, New exact solutions for free vibrations of rectangular thin plates by symplectic dual method, *Acta Mechanica Sinica*, 25, 265-270, 2009.
- [17] Sh. Hosseini-Hashemi, H. Salehipour and S.R. Atashipour, Exact three-dimensional free vibration analysis of thick homogeneous plates coated by a functionally graded layer, *Acta Mechanica*, 223, 2153-2166, 2012.
- [18] S.S. Vel and R.C. Batra, Three-dimensional exact solution for the vibration of functionally graded rectangular plates, *Journal of Sound and Vibration*, 272, 703-730, 2004.
- [19] Y. Xu and D. Zhou, Three-dimensional elasticity solution of functionally graded rectangular plates with variable thickness, *Composite Structures*, 91, 56-65, 2009.

- [20] D. Haojiang, X. Rongqiao and C. Weiqiu, Exact solutions for free vibration of transversely isotropic piezoelectric circular plates, *Acta Mechanica Sinica*, 16, 142-147, 2000.
- [21] B.P. Baillargeon and S.S. Vel, Exact solution for the vibration and active damping of composite plates with piezoelectric shear actuators, *Journal of Sound and Vibration*, 282, 781-804, 2005.
- [22] W.Q. Chen, J.B. Cai, G.R. Ye and Y.F. Wang, Exact three-dimensional solutions of laminated orthotropic piezoelectric rectangular plates featuring interlaminar bonding imperfections modeled by a general spring layer, *International Journal of Solids and Structures*, 41, 5247-5263, 2004.
- [23] Z.-Q. Cheng, C.W. Lim and S. Kitipornchai, Three-dimensional exact solution for inhomogeneous and laminated piezoelectric plates, *International Journal of Engineering Science*, 37, 1425-1439, 1999.
- [24] S. Kapuria and P.G. Nair, Exact three-dimensional piezothermoelasticity solution for dynamics of rectangular cross-ply hybrid plates featuring interlaminar bonding imperfections, *Composites Science and Technology*, 70, 752-762, 2010.
- [25] Z. Zhong and E.T. Shang, Three-dimensional exact analysis of a simply supported functionally gradient piezoelectric plate, *International Journal of Solids and Structures*, 40, 5335-5352, 2003.
- [26] W.-Q. Chen, H.-J. Ding and R.-Q. Xu, On exact analysis of free vibrations of embedded transversely isotropic cylindrical shells, *International Journal of Pressure Vessels and Piping*, 75, 961-966, 1998.
- [27] J.-R. Fan and J.-Y. Zhang, Exact solutions for thick laminated shells, *Science in China*, 35, 1343-1355, 1992.
- [28] B. Gasemzadeh, R. Azarafza, Y. Sahebi and A. Motallebi, Analysis of free vibration of cylindrical shells on the basis of three dimensional exact elasticity theory, *Indian Journal of Science and Technology*, 5, 3260-3262, 2012.
- [29] N.N. Huang, Exact analysis for three-dimensional free vibrations of cross-ply cylindrical and doubly-curved laminates, *Acta Mechanica*, 108, 23-34, 1995.
- [30] J.N. Sharma, D.K. Sharma and S.S. Dhaliwal, Three-dimensional free vibration analysis of a viscothermoelastic hollow sphere, *Open Journal of Acoustics*, 2, 12-24, 2012.
- [31] J.N. Sharma and N. Sharma, Three-dimensional free vibration analysis of a homogeneous transversally isotropic thermoelastic sphere, *Journal of Applied Mechanics*, 77, 1-9, 2010.
- [32] K.P. Soldatos and J. Ye, Axisymmetric static and dynamic analysis of laminated hollow cylinders composed of monoclinic elastic layers, *Journal of Sound and Vibration*, 184, 245-259, 1995.
- [33] A.E. Armenakas, D.C. Gazis and G. Herrmann, *Free Vibrations of Circular Cylindrical Shells*, Pergamon Press, Oxford, 1969.
- [34] A. Bhimaraddi, A higher order theory for free vibration analysis of circular cylindrical shells, *International Journal of Solids and Structures*, 20, 623-630, 1984.
- [35] H. Zhou, W. Li, B. Lv and W.L. Li, Free vibrations of cylindrical shells with elastic-support boundary conditions, *Applied Acoustics*, 73, 751-756, 2012.
- [36] S.M.R. Khalili, A. Davar and K.M. Fard, Free vibration analysis of homogeneous isotropic circular cylindrical shells based on a new three-dimensional refined higher-order theory, *International Journal of Mechanical Sciences*, 56, 1-25, 2012.

- [37] S.S. Vel, Exact elasticity solution for the vibration of functionally graded anisotropic cylindrical shells, *Composite Structures*, 92, 2712-2727, 2010.
- [38] C.T. Loy and K.Y. Lam, Vibration of thick cylindrical shells on the basis of three-dimensional theory of elasticity, *Journal of Sound and Vibration*, 226, 719-737, 1999.
- [39] Y. Wang, R. Xu, H. Ding and J. Chen, Three-dimensional exact solutions for free vibrations of simply supported magneto-electro-elastic cylindrical panels, *International Journal of Engineering Science*, 48, 1778-1796, 2010.
- [40] E. Efraim and M. Eisenberger, Exact vibration frequencies of segmented axisymmetric shells, *Thin-Walled Structures*, 44, 281-289, 2006.
- [41] J.-H. Kanga and A.W. Leissa, Three-dimensional vibrations of thick spherical shell segments with variable thickness, *International Journal of Solids and Structures*, 37, 4811-4823, 2000.
- [42] K.M. Liew, L.X. Peng and T.Y. Ng, Three-dimensional vibration analysis of spherical shell panels subjected to different boundary conditions, *International Journal of Mechanical Sciences*, 44, 2103-2117, 2002.
- [43] A.W. Leissa, *Vibration of Plates*, NASA SP-160, Washington, 1969.
- [44] A.W. Leissa, *Vibration of Shells*, NASA SP-288, Washington, 1973.
- [45] F.B. Hildebrand, E. Reissner and G.B. Thomas, *Notes on the Foundations of the Theory of Small Displacements of Orthotropic Shells*, NACA Technical Note No. 1833, Washington, 1949.
- [46] F. Tornabene, *Meccanica delle Strutture a Guscio in Materiale Composito*, Società Editrice Esculapio, Bologna (Italy), 2012.
- [47] W. Soedel, *Vibration of Shells and Plates*, Marcel Dekker, Inc., New York, 2004.
- [48] Open document, *Systems of Differential Equations*, free available on <http://www.math.utah.edu/gustafso/>, accessed on 23rd May 2013.
- [49] W.E. Boyce and R.C. DiPrima, *Elementary Differential Equations and Boundary Value Problems*, John Wiley & Sons, Ltd., New York, 2001.
- [50] D. Zwillinger, *Handbook of Differential Equations*, Academic Press, New York, 1997.
- [51] C. Molery and C. Van Loan, Nineteen dubious ways to compute the exponential of a matrix, twenty-five years later, *SIAM Review*, 45, 1-46, 2003.

Mode	I	II	III	
$0^\circ/90^\circ$				
3D[10]	0.060274	0.52994	0.58275	(1,1)
Present 3D	0.060274	0.52994	0.58275	(1,1)
3D[10]	0.14539	0.62352	0.95652	(1,2)
Present 3D	0.14538	0.62352	0.95652	(1,2)
3D[10]	0.14539	0.62352	0.95652	(2,1)
Present 3D	0.14538	0.62352	0.95652	(2,1)
3D[10]	0.20229	0.95796	1.0300	(2,2)
Present 3D	0.20229	0.95796	1.0300	(2,2)
$0^\circ/90^\circ/0^\circ$				
3D[10]	0.067147	0.50349	0.63775	(1,1)
Present 3D	0.067147	0.50349	0.63775	(1,1)
3D[10]	0.12811	0.6888	0.95017	(1,2)
Present 3D	0.12811	0.6888	0.95017	(1,2)
3D[10]	0.17217	0.58366	1.1780	(2,1)
Present 3D	0.17217	0.58366	1.1780	(2,1)
3D[10]	0.20798	0.97517	1.2034	(2,2)
Present 3D	0.20798	0.97517	1.2034	(2,2)
$0^\circ/90^\circ/0^\circ/90^\circ$				
3D[10]	0.066210	0.54596	0.59996	(1,1)
Present 3D	0.066210	0.54596	0.59995	(1,1)
3D[10]	0.15194	0.63875	1.0761	(1,2)
Present 3D	0.15194	0.63875	1.0761	(1,2)
3D[10]	0.15194	0.63875	1.0761	(2,1)
Present 3D	0.15194	0.63875	1.0761	(2,1)
3D[10]	0.20841	1.0623	1.1557	(2,2)
Present 3D	0.20841	1.0623	1.1557	(2,2)

Table 1: Assessment 1. Simply supported multilayered composite square plate. First three exact natural circular frequencies in no-dimensional form  $\bar{\omega} = \omega h \sqrt{\frac{\rho}{E_2}}$  for various half-wave numbers (m,n) imposed. Comparison between present three-dimensional analysis and three-dimensional analysis by Messina [10] for thickness ratio a/h=10.

m,n	mode	$N_L = 2$		$N_L = 4$		$N_L = 10$	
		3D[29]	Present 3D	3D[29]	Present 3D	3D[29]	Present 3D
1,1	I	1.8971	1.8971	2.3415	2.3415	2.4930	2.4930
1,1	II	18.813	18.813	21.545	21.545	22.387	22.387
1,1	III	20.169	20.169	22.902	22.902	23.694	23.694
1,2	I	4.4492	4.4492	4.9620	4.9620	5.3017	5.3017
1,3	I	7.8195	7.8195	8.0752	8.0753	8.5254	8.5253
2,1	I	4.3485	4.3485	4.8493	4.8493	5.1853	5.1853
2,2	I	6.0384	6.0384	6.5486	6.5486	6.9739	6.9739
2,3	I	8.8895	8.8895	9.1438	9.1438	9.6347	9.6346
3,1	I	7.7503	7.7503	7.9573	7.9573	8.3952	8.3950
3,2	I	8.9012	8.9012	9.1290	9.1290	9.6122	9.6120
3,3	I	11.103	11.103	11.164	11.164	11.686	11.686

Table 2: Assessment 2. Simply supported multilayered composite cylindrical shell panel. Modes versus half-wave numbers (m,n) for several layers ( $N_L$ ) and lamination sequence ( $0^\circ/90^\circ/0^\circ/90^\circ/\dots$ ). Comparison between present three-dimensional analysis and three-dimensional analysis by Huang [29] in term of no-dimensional circular frequencies  $\bar{\omega} = \omega R_\alpha \sqrt{\frac{\rho}{E_0}}$  for thickness ratio  $R_\alpha/h = 20$ .

m,n	mode	$N_L = 2$		$N_L = 4$		$N_L = 10$	
		3D[29]	Present 3D	3D[29]	Present 3D	3D[29]	Present 3D
1,1	I	4.6238	4.6240	5.8070	5.8070	6.2293	6.2293
1,2	I	10.753	10.753	12.134	12.134	13.050	13.050
1,3	I	19.130	19.130	19.846	19.845	21.042	21.042
2,1	I	10.864	10.864	12.188	12.188	13.076	13.076
2,2	I	14.909	14.909	16.298	16.298	17.432	17.432
2,3	I	21.961	21.961	22.719	22.719	24.027	24.027
3,1	I	19.315	19.315	19.932	19.931	21.082	21.081
3,2	I	22.053	22.053	22.757	22.757	24.045	24.045
3,3	I	27.483	27.483	27.790	27.790	29.189	29.189

Table 3: Assessment 3. Simply supported multilayered composite spherical shell panel. Modes versus half-wave numbers (m,n) for several layers ( $N_L$ ) and lamination sequence ( $0^\circ/90^\circ/0^\circ/90^\circ/\dots$ ). Comparison between present three-dimensional analysis and three-dimensional analysis by Huang [29] in term of no-dimensional circular frequencies  $\bar{\omega} = \omega R_\alpha \sqrt{\frac{\rho}{E_0}}$  for thickness ratio  $R_\alpha/h = 50$ .

a/h	100	50	10	5
		(m = 0, n = 1)		
I mode	4.2035	3.8748	1.6497	0.9451
II mode	191.42	95.707	19.133	6.9370
III mode	323.64	161.80	23.325	9.5516
		(m = 1, n = 0)		
I mode	4.2035	3.8748	1.6497	0.9451
II mode	191.42	95.707	19.133	6.9370
III mode	323.64	161.80	23.325	9.5516
		(m = 1, n = 1)		
I mode	8.1693	7.0764	2.4879	1.4786
II mode	270.70	135.35	27.045	6.8059
III mode	457.67	228.77	28.081	13.473
		(m = 1, n = 2)		
I mode	18.908	14.477	4.3479	2.8767
II mode	428.01	213.99	27.596	6.7271
III mode	723.55	361.48	42.691	20.972
		(m = 2, n = 1)		
I mode	18.908	14.477	4.3479	2.8767
II mode	428.01	213.99	27.596	6.7271
III mode	723.55	361.48	42.691	20.972
		(m = 2, n = 2)		
I mode	28.306	20.121	5.9146	4.1973
II mode	541.39	270.67	27.223	7.0358
III mode	915.10	425.01	53.891	25.225

Table 4: Benchmark 1. Simply supported sandwich square plate with isotropic skins. First three vibration modes in term of no-dimensional circular frequency  $\bar{\omega} = \omega \frac{a^2}{h} \sqrt{\frac{\rho_{skin}}{E_{skin}}}$  for several combinations of half-wave numbers m and n.



a/h	100	50	10	5
		(m = 0, n = 1)		
I mode	9.4566	8.7778	3.8148	2.1100
II mode	222.85	111.42	22.282	11.136
III mode	786.78	393.31	40.545	14.091
		(m = 1, n = 0)		
I mode	10.978	10.186	4.4056	2.4091
II mode	222.85	111.42	22.282	11.136
III mode	786.77	393.28	40.555	14.092
		(m = 1, n = 1)		
I mode	15.754	14.440	5.9275	3.2639
II mode	771.58	385.73	71.631	17.398
III mode	861.39	430.56	76.817	37.351
		(m = 1, n = 2)		
I mode	38.540	31.191	9.6637	5.5954
II mode	897.28	448.53	70.874	16.773
III mode	1592.9	795.70	89.723	43.039
		(m = 2, n = 1)		
I mode	43.343	34.853	10.471	5.9335
II mode	897.30	448.57	70.630	16.538
III mode	1592.7	795.38	89.454	43.079
		(m = 2, n = 2)		
I mode	57.761	45.175	13.056	7.6556
II mode	1542.9	771.00	69.593	16.392
III mode	1722.2	859.78	149.40	52.297

Table 5: Benchmark 2. Simply supported sandwich square plate with composite skins. First three vibration modes in term of no-dimensional circular frequency  $\bar{\omega} = \omega \frac{a^2}{h} \sqrt{\frac{\rho_{skin}}{E_{2skin}}}$  for several combinations of half-wave numbers m and n.

a/h	100	50	10	5
		(m = 0, n = 1)		
I mode	0.4798	0.4749	0.3700	0.2499
II mode	63.806	31.903	6.3803	3.1896
III mode	107.88	53.941	10.783	4.5804
		(m = 1, n = 0)		
I mode	4.2035	3.8748	1.6497	0.9451
II mode	191.42	95.707	19.133	6.9370
III mode	323.64	161.80	23.325	9.5516
		(m = 1, n = 1)		
I mode	4.6553	4.2583	1.7567	1.0092
II mode	201.77	100.88	20.167	6.9197
III mode	341.14	170.55	24.201	10.066
		(m = 1, n = 2)		
I mode	5.9935	5.3640	2.0524	1.1925
II mode	230.05	115.02	22.990	6.8719
III mode	388.96	194.44	26.659	11.467
		(m = 2, n = 1)		
I mode	15.886	12.529	3.8450	2.4756
II mode	388.11	194.04	27.731	6.7050
III mode	656.12	327.85	38.731	19.141
		(m = 2, n = 2)		
I mode	17.033	13.278	4.0367	2.6268
II mode	403.53	201.75	27.679	6.7091
III mode	682.19	340.85	40.263	19.859

Table 6: Benchmark 3. Simply supported sandwich rectangular plate with isotropic skins. First three vibration modes in term of no-dimensional circular frequency  $\bar{\omega} = \omega \frac{a^2}{h} \sqrt{\frac{\rho_{skin}}{E_{skin}}}$  for several combinations of half-wave numbers m and n.

a/h	100	50	10	5
		(m = 0, n = 1)		
I mode	1.0767	1.0667	0.8467	0.5788
II mode	74.284	37.142	7.4283	3.7140
III mode	262.28	131.13	26.207	9.2196
		(m = 1, n = 0)		
I mode	10.978	10.186	4.4056	2.4091
II mode	222.85	111.42	22.282	11.136
III mode	786.77	393.28	40.555	14.092
		(m = 1, n = 1)		
I mode	11.231	10.421	4.5385	2.4968
II mode	342.45	171.22	34.219	19.965
III mode	791.01	395.40	48.469	17.876
		(m = 1, n = 2)		
I mode	12.500	11.596	5.0608	2.7888
II mode	563.40	281.68	56.150	17.593
III mode	805.27	402.52	66.581	27.916
		(m = 2, n = 1)		
I mode	40.944	32.851	9.7156	5.4768
II mode	516.10	258.04	51.546	16.689
III mode	1575.2	786.66	62.312	25.699
		(m = 2, n = 2)		
I mode	41.684	33.470	9.9872	5.6419
II mode	684.88	342.41	67.861	16.625
III mode	1581.6	789.84	71.505	33.814

Table 7: Benchmark 4. Simply supported sandwich rectangular plate with composite skins. First three vibration modes in term of no-dimensional circular frequency  $\bar{\omega} = \omega \frac{a^2}{h} \sqrt{\frac{\rho_{skin}}{E_{2skin}}}$  for several combinations of half-wave numbers m and n.

$R_\alpha/h$	1000	100	10	5
		$(m = 0, n = 1)$		
I mode	1048.5	104.85	10.495	5.2469
II mode	1049.6	104.96	10.513	5.2612
III mode	1823.8	182.38	17.822	6.4256
		$(m = 1, n = 0)$		
I mode	3.4655	3.5522	1.4329	0.8259
II mode	2004.5	200.45	19.922	7.2736
III mode	3572.6	357.23	24.975	9.5143
		$(m = 1, n = 1)$		
I mode	218.88	22.345	2.7559	1.4630
II mode	2323.0	232.30	23.080	7.2572
III mode	3948.2	394.78	26.028	11.201
		$(m = 1, n = 2)$		
I mode	543.31	54.875	5.9407	3.0639
II mode	2978.4	297.84	28.837	7.7248
III mode	4961.8	496.13	29.800	14.505
		$(m = 2, n = 1)$		
I mode	70.375	17.298	3.9690	2.5498
II mode	4156.6	415.66	30.015	7.2912
III mode	7089.8	708.82	40.829	19.404
		$(m = 2, n = 2)$		
I mode	229.38	29.488	4.9357	3.1081
II mode	4557.8	455.78	29.953	7.3789
III mode	7712.0	771.00	44.892	21.465

Table 8: Benchmark 5. Simply supported sandwich cylindrical shell panel with isotropic skins. First three vibration modes in term of no-dimensional circular frequency  $\bar{\omega} = \omega \frac{a^2}{h} \sqrt{\frac{\rho_{skin}}{E_{skin}}}$  for several combinations of half-wave numbers m and n.

$R_\alpha/h$	1000	100	10	5
		$(m = 0, n = 1)$		
I mode	1221.9	122.19	12.220	6.1109
II mode	2743.2	274.33	27.534	11.237
III mode	4316.5	431.64	39.076	13.803
		$(m = 1, n = 0)$		
I mode	9.4940	9.2744	3.8297	2.1105
II mode	2333.7	233.37	23.322	11.470
III mode	8685.4	868.42	43.955	15.367
		$(m = 1, n = 1)$		
I mode	338.13	35.247	5.4162	2.9011
II mode	4875.2	487.52	48.665	18.627
III mode	8781.1	877.98	61.782	24.208
		$(m = 1, n = 2)$		
I mode	723.96	73.860	9.1701	4.7742
II mode	8488.9	848.83	73.279	18.752
III mode	9419.3	941.81	84.391	40.481
		$(m = 2, n = 1)$		
I mode	143.15	42.140	9.9226	5.6055
II mode	6334.6	633.45	63.059	18.218
III mode	16759	1675.2	74.258	30.815
		$(m = 2, n = 2)$		
I mode	354.29	54.967	11.148	6.2612
II mode	9736.1	973.56	76.774	18.147
III mode	16924	1691.7	96.967	46.652

Table 9: Benchmark 6. Simply supported sandwich cylindrical shell panel with composite skins. First three vibration modes in term of no-dimensional circular frequency  $\bar{\omega} = \omega \frac{a^2}{h} \sqrt{\frac{\rho_{skin}}{E_{2skin}}}$  for several combinations of half-wave numbers m and n.

$R_\alpha/h$	1000	100	10	5
		$(m = 0, n = 1)$		
I mode	7556.8	755.69	75.574	37.795
II mode	12128	1212.8	121.27	60.629
III mode	40870	4087.1	409.55	135.88
		$(m = 2, n = 1)$		
I mode	2403.4	240.34	24.098	12.125
II mode	26792	2679.3	267.96	132.95
III mode	58169	5816.8	564.63	176.45
		$(m = 2, n = 2)$		
I mode	7577.9	757.81	75.989	38.143
II mode	32790	3279.0	327.93	162.44
III mode	60297	6029.5	577.50	181.27
		$(m = 2, n = 3)$		
I mode	13301	1330.1	133.43	66.873
II mode	39378	3937.8	393.70	189.93
III mode	64363	6436.2	602.43	199.82

Table 10: Benchmark 7. Simply supported sandwich cylinder with isotropic skins. First three vibration modes in term of no-dimensional circular frequency  $\bar{\omega} = \omega \frac{a^2}{h} \sqrt{\frac{\rho_{skin}}{E_{skin}}}$  for several combinations of half-wave numbers m and n.

$R_\alpha/h$	1000	100	10	5
		$(m = 0, n = 1)$		
I mode	8797.8	879.79	87.986	44.004
II mode	31038	3103.8	310.42	155.25
III mode	98885	9888.8	991.38	340.44
		$(m = 2, n = 1)$		
I mode	4597.4	459.76	46.133	23.238
II mode	41954	4195.4	419.69	209.84
III mode	139995	13999	1376.7	395.64
		$(m = 2, n = 2)$		
I mode	11287	1128.7	113.47	57.169
II mode	68111	6811.1	681.10	340.25
III mode	140500	14049	1382.3	473.05
		$(m = 2, n = 3)$		
I mode	17724	1772.6	178.60	89.936
II mode	96930	9693.0	968.91	481.89
III mode	141452	14145	1392.4	500.05

Table 11: Benchmark 8. Simply supported sandwich cylinder with composite skins. First three vibration modes in term of no-dimensional circular frequency  $\bar{\omega} = \omega \frac{a^2}{h} \sqrt{\frac{\rho_{skin}}{E_{2skin}}}$  for several combinations of half-wave numbers m and n.

$R_\alpha/h$	1000	100	10	5
		$(m = 0, n = 1)$		
I mode	981.60	98.206	9.8978	4.9418
II mode	2004.5	200.44	19.832	8.6325
III mode	3720.6	372.02	25.094	9.4554
		$(m = 1, n = 0)$		
I mode	981.60	98.206	9.8978	4.9418
II mode	2004.5	200.44	19.832	8.6325
III mode	3720.6	372.02	25.094	9.4554
		$(m = 1, n = 1)$		
I mode	1028.2	103.05	10.522	5.2854
II mode	2834.8	283.47	27.909	8.9414
III mode	5023.6	502.27	31.006	13.256
		$(m = 1, n = 2)$		
I mode	1057.7	107.25	11.397	5.9281
II mode	4482.2	448.19	31.688	9.1047
III mode	7722.5	772.01	43.743	20.734
		$(m = 2, n = 1)$		
I mode	1057.7	107.25	11.397	5.9281
II mode	4482.2	448.19	31.688	9.1045
III mode	7722.5	772.01	43.743	20.734
		$(m = 2, n = 2)$		
I mode	1065.5	110.00	12.169	6.6340
II mode	5669.6	566.92	31.542	9.4322
III mode	9699.6	969.53	55.069	25.826

Table 12: Benchmark 9. Simply supported sandwich spherical shell panel with isotropic skins. First three vibration modes in term of no-dimensional circular frequency  $\bar{\omega} = \omega \frac{a^2}{h} \sqrt{\frac{\rho_{skin}}{E_{skin}}}$  for several combinations of half-wave numbers m and n.

$R_\alpha/h$	1000	100	10	5
		$(m = 0, n = 1)$		
I mode	2333.7	233.36	23.205	11.290
II mode	2578.7	257.96	25.978	12.974
III mode	8769.8	876.85	44.188	15.622
		$(m = 1, n = 0)$		
I mode	2333.7	233.36	23.205	11.290
II mode	2578.7	258.00	26.045	12.994
III mode	8769.8	876.84	44.199	15.624
		$(m = 1, n = 1)$		
I mode	1338.4	134.45	14.290	7.2379
II mode	8080.3	807.96	72.088	19.204
III mode	9760.1	975.81	79.253	37.348
		$(m = 1, n = 2)$		
I mode	1619.3	165.77	18.611	9.6555
II mode	9618.2	961.70	75.850	19.742
III mode	16948	1694.2	95.578	44.582
		$(m = 2, n = 1)$		
I mode	1619.4	166.83	19.045	9.8596
II mode	9618.2	961.73	75.709	19.558
III mode	16948	1694.1	94.776	44.019
		$(m = 2, n = 2)$		
I mode	1419.9	152.27	19.172	10.310
II mode	16161	1615.7	76.611	19.207
III mode	18417	1840.8	154.39	56.868

Table 13: Benchmark 10. Simply supported sandwich spherical shell panel with composite skins. First three vibration modes in term of no-dimensional circular frequency  $\bar{\omega} = \omega \frac{a^2}{h} \sqrt{\frac{\rho_{skin}}{E_{2skin}}}$  for several combinations of half-wave numbers m and n.



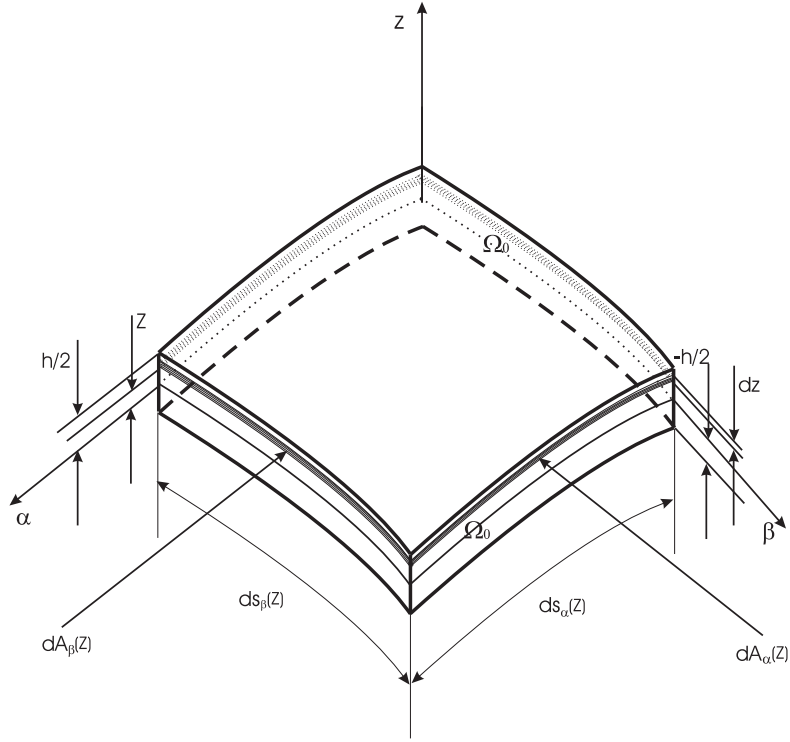


Figure 1: Geometry, notation and reference system for shells.

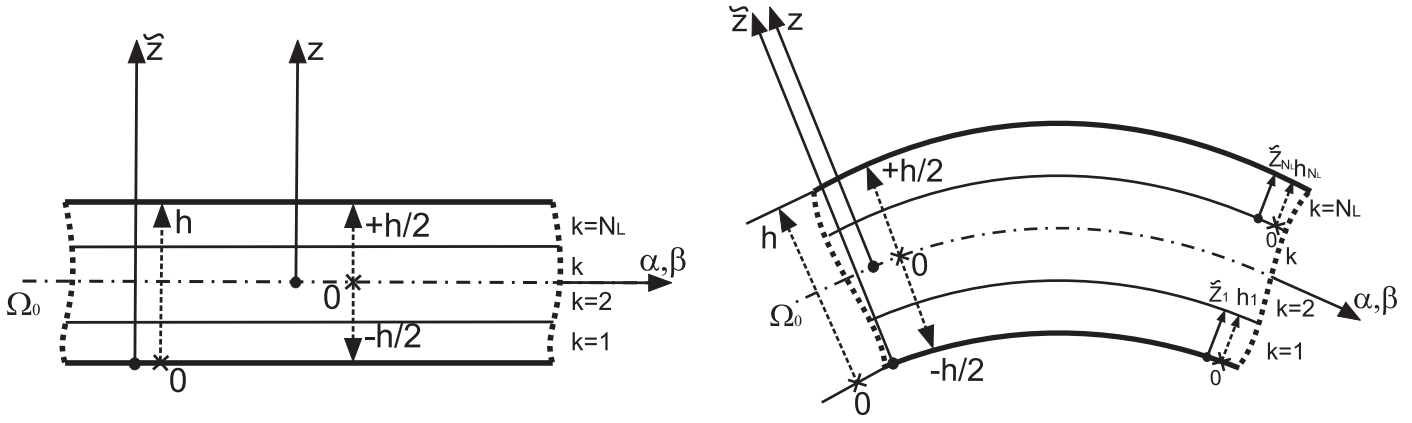


Figure 2: Thickness coordinates and reference systems for plates and shells.

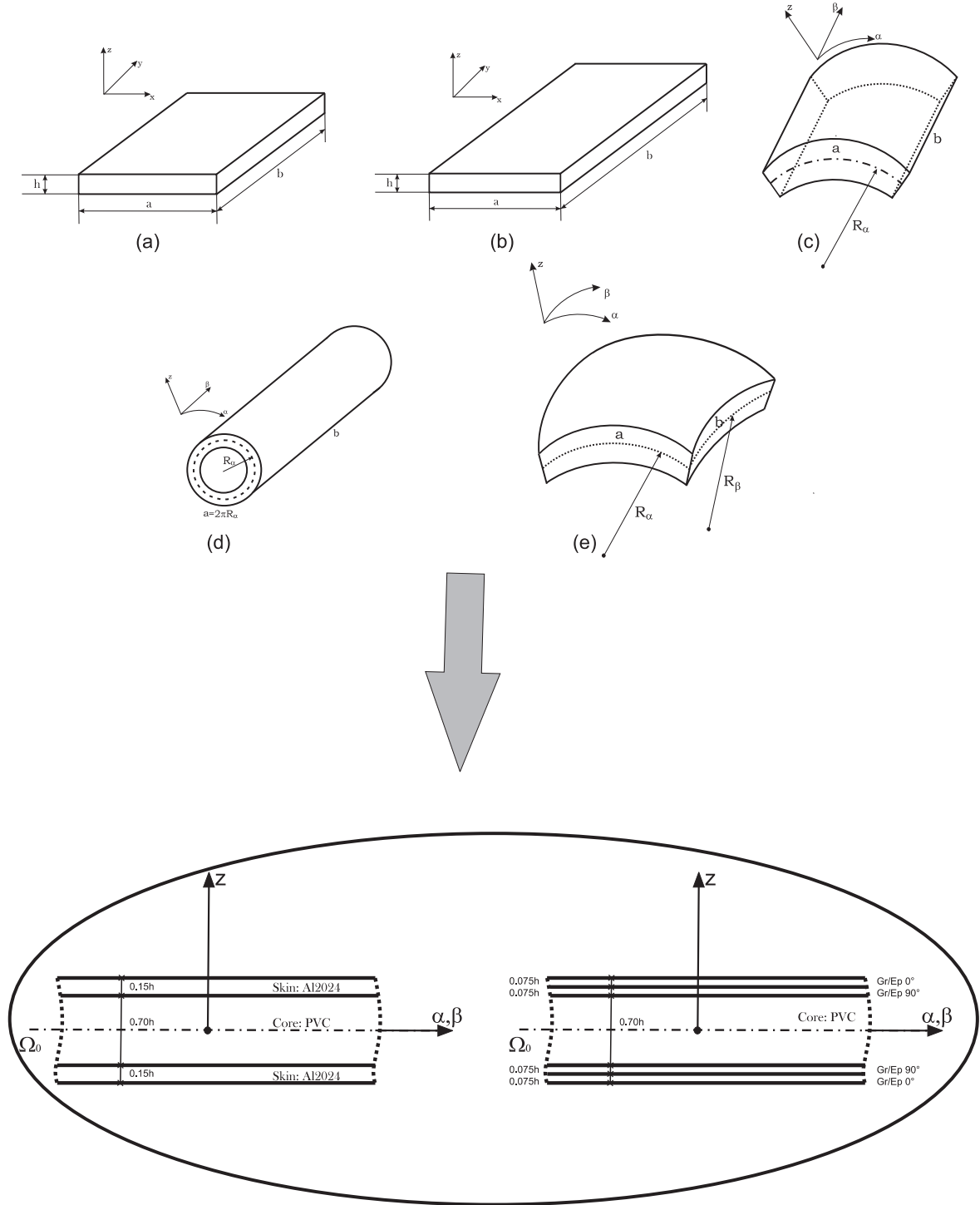


Figure 3: Geometries and lamination sequences considered for the assessments and benchmarks: (a) square plate, (b) rectangular plate, (c) cylindrical shell panel, (d) cylinder, (e) spherical shell panel.

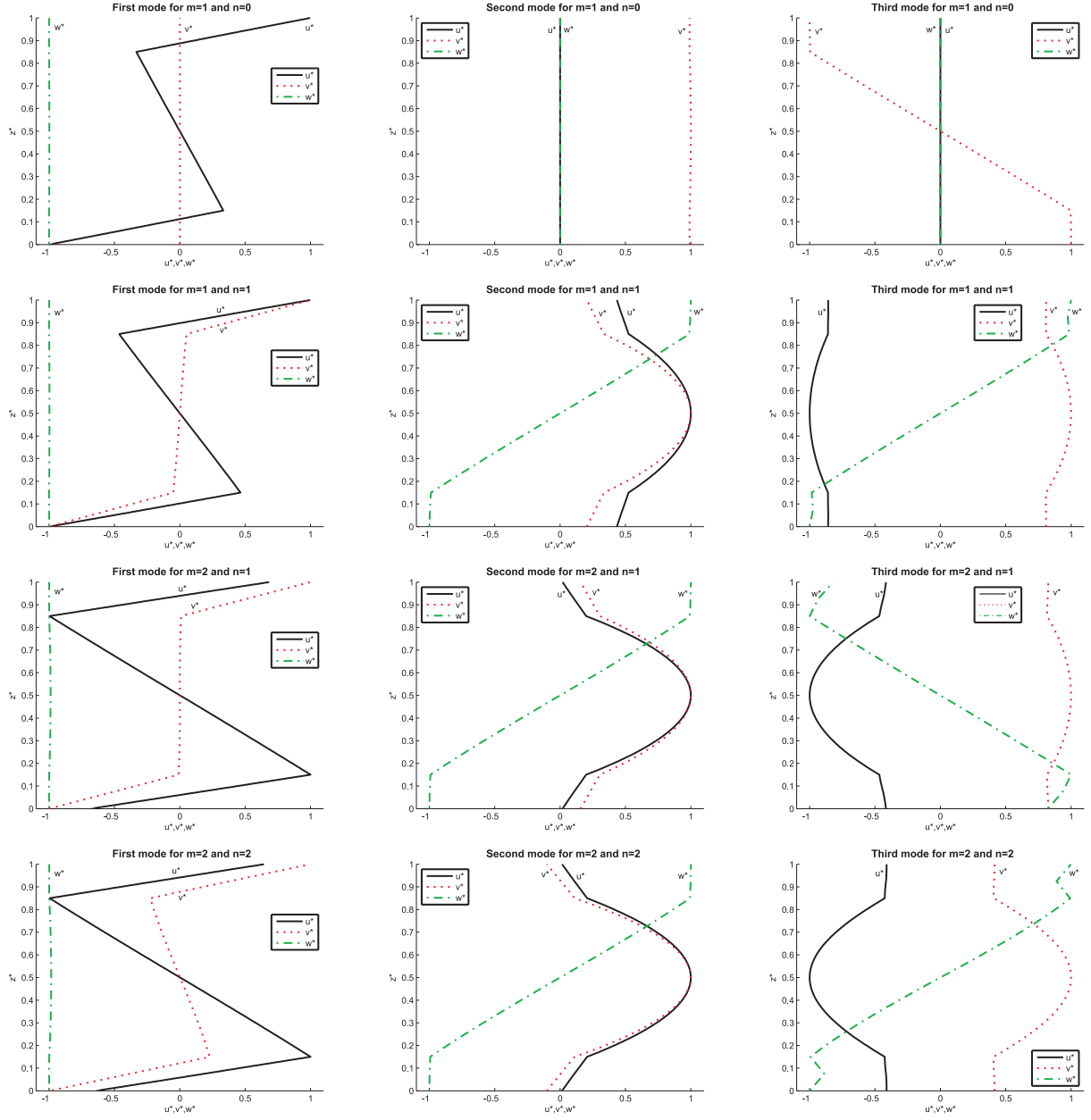


Figure 4: Benchmark 2, simply supported sandwich square plate with composite faces and thickness ratio  $a/h=10$ . First three vibration modes in terms of displacement components through the thickness for several combinations of half-wave numbers.

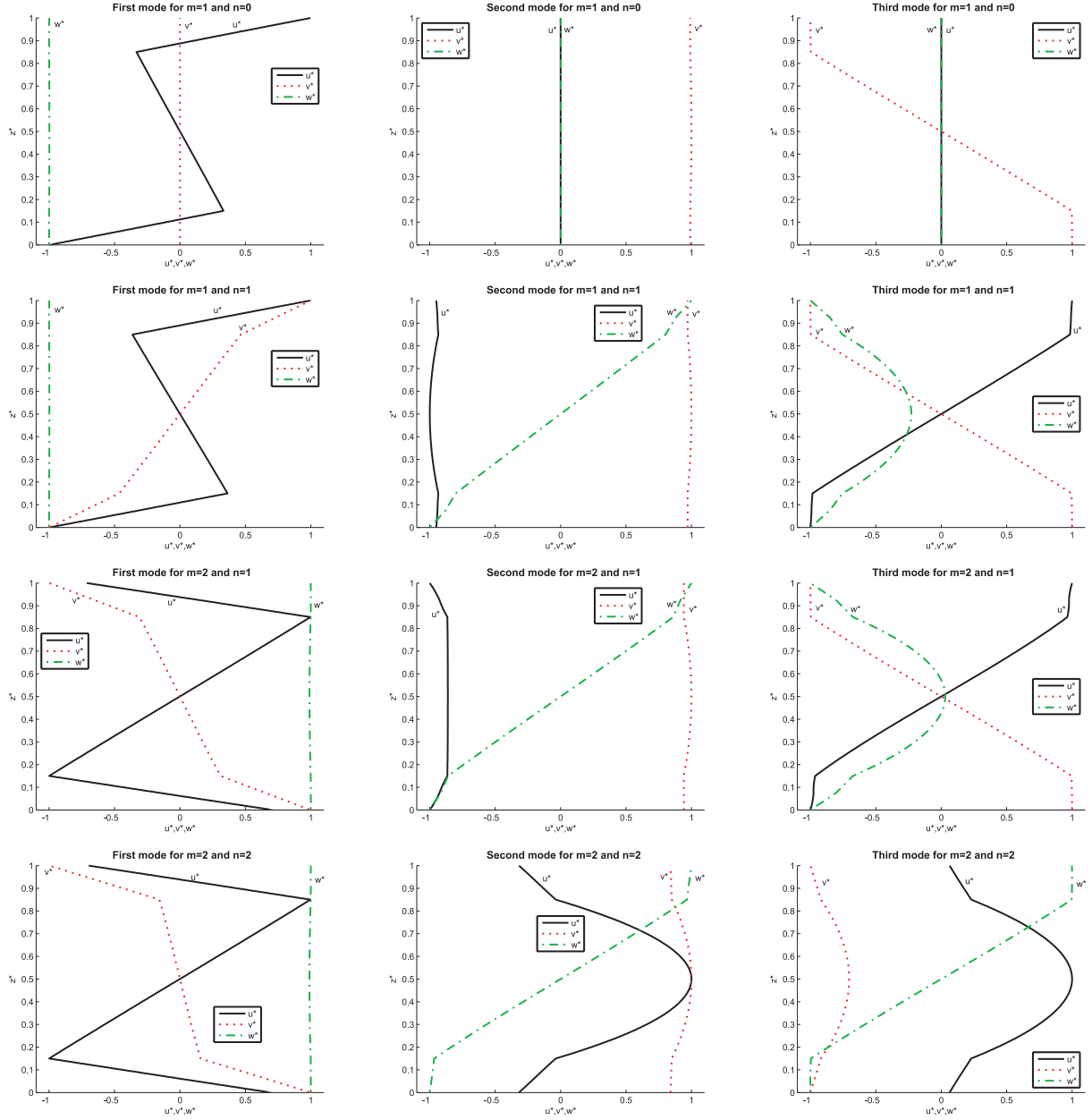


Figure 5: Benchmark 4, simply supported sandwich rectangular plate with composite faces and thickness ratio  $a/h=10$ . First three vibration modes in terms of displacement components through the thickness for several combinations of half-wave numbers.

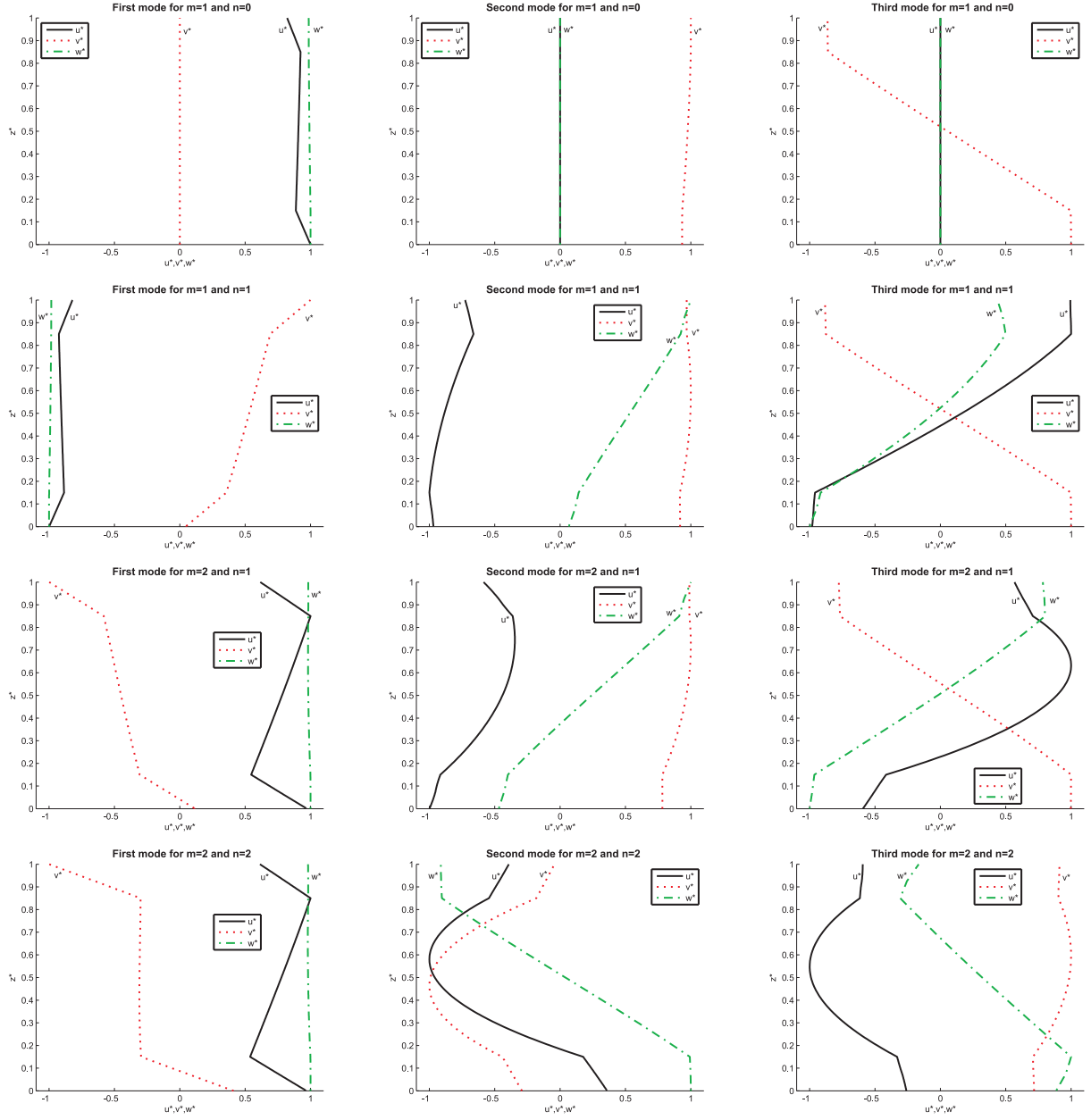


Figure 6: Benchmark 6, simply supported sandwich cylindrical shell panel with composite faces and thickness ratio  $R_\alpha/h = 10$ . First three vibration modes in terms of displacement components through the thickness for several combinations of half-wave numbers.

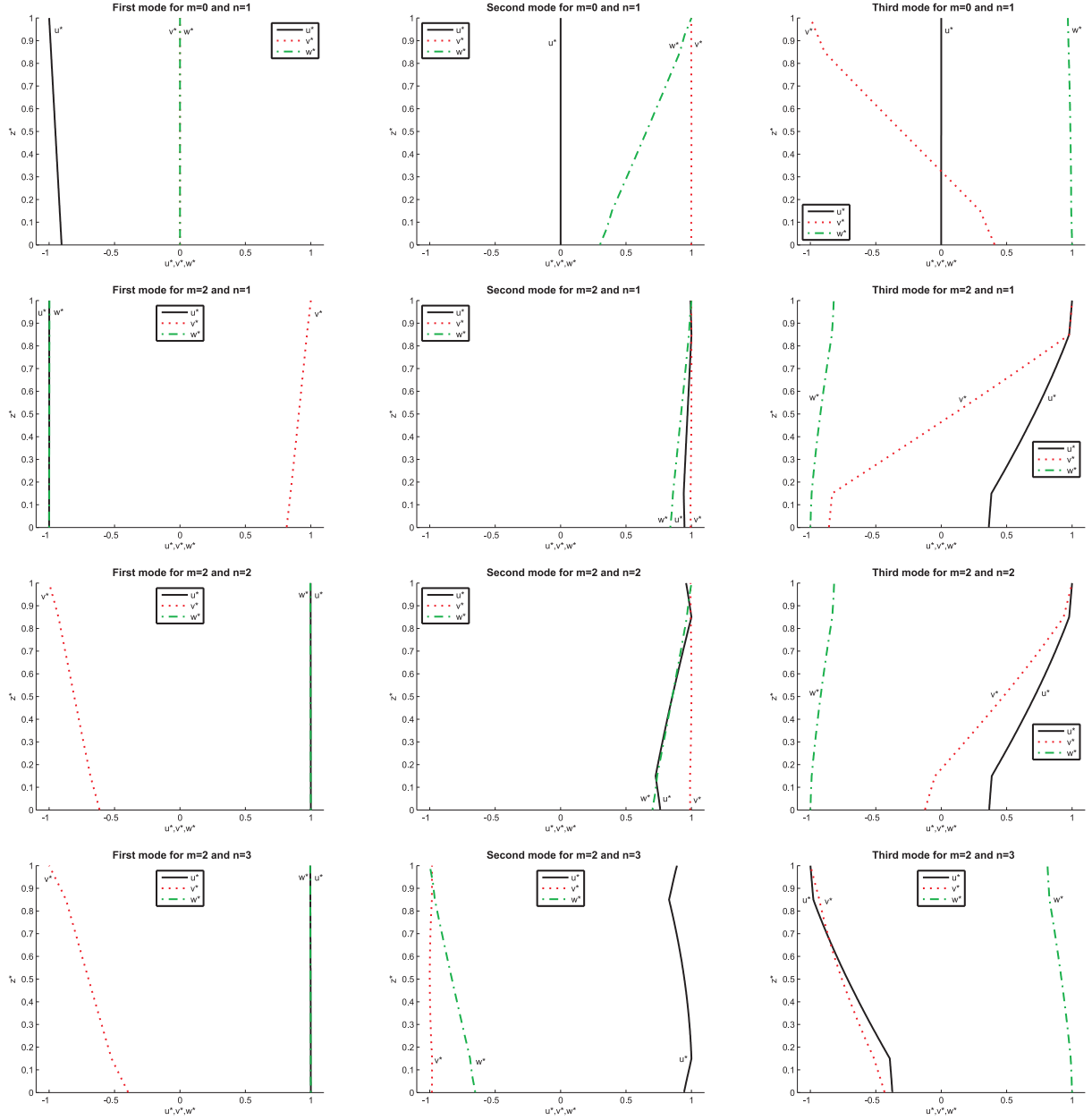


Figure 7: Benchmark 8, simply supported sandwich cylinder with composite faces and thickness ratio  $R_\alpha/h = 10$ . First three vibration modes in terms of displacement components through the thickness for several combinations of half-wave numbers.

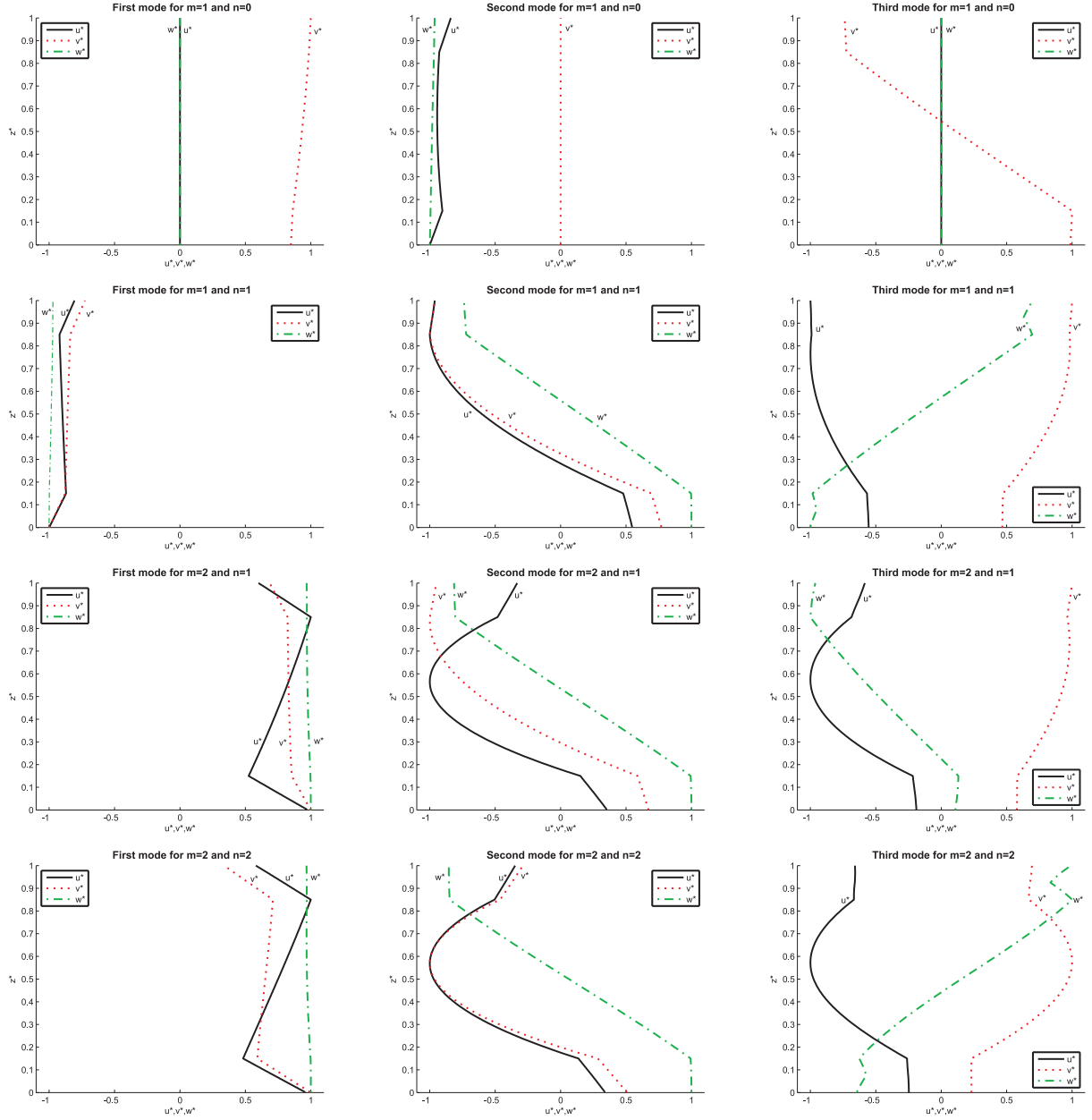


Figure 8: Benchmark 10, simply supported sandwich spherical shell panel with composite faces and thickness ratio  $R_\alpha/h = 10$ . First three vibration modes in terms of displacement components through the thickness and several combinations of half-wave numbers.

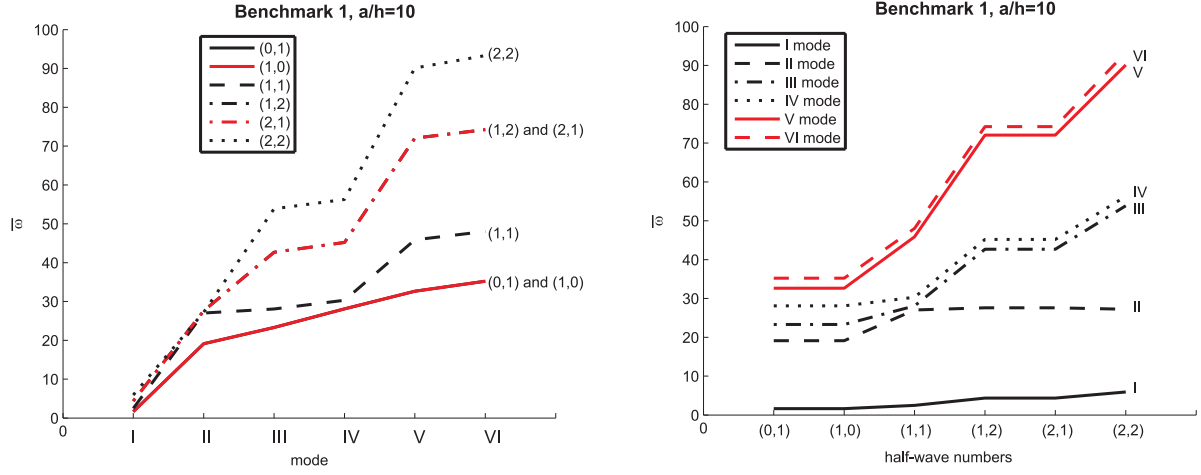


Figure 9: Benchmark 1, simply supported sandwich square plate with isotropic faces and thickness ratio  $a/h=10$ . No-dimensional circular frequencies versus mode order and half-wave numbers.

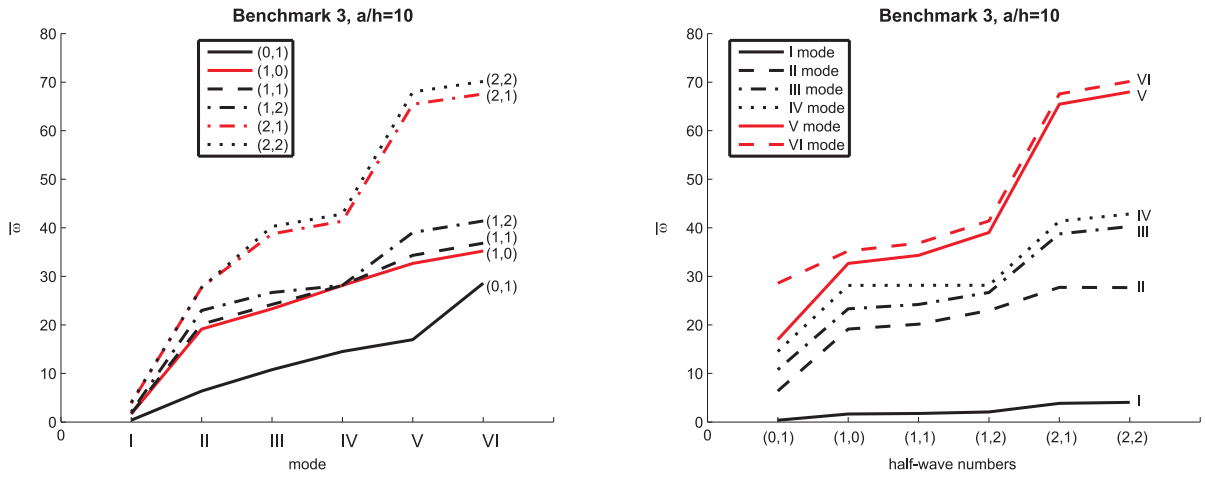


Figure 10: Benchmark 3, simply supported sandwich rectangular plate with isotropic faces and thickness ratio  $a/h=10$ . No-dimensional circular frequencies versus mode order and half-wave numbers.



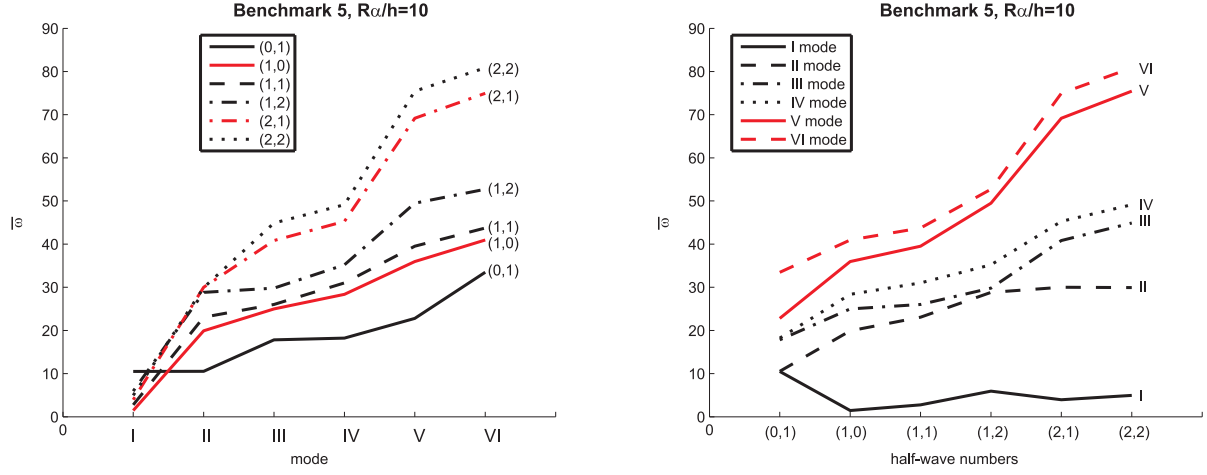


Figure 11: Benchmark 5, simply supported sandwich cylindrical shell panel with isotropic faces and thickness ratio  $R_\alpha/h = 10$ . No-dimensional circular frequencies versus mode order and half-wave numbers.

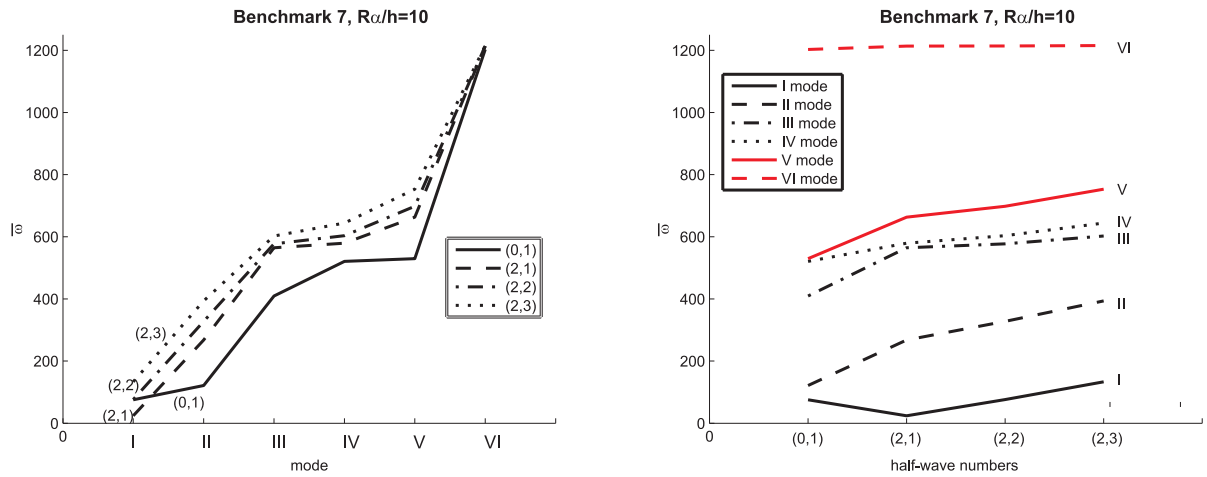


Figure 12: Benchmark 7, simply supported sandwich cylinder with isotropic faces and thickness ratio  $R_\alpha/h = 10$ . No-dimensional circular frequencies versus mode order and half-wave numbers.

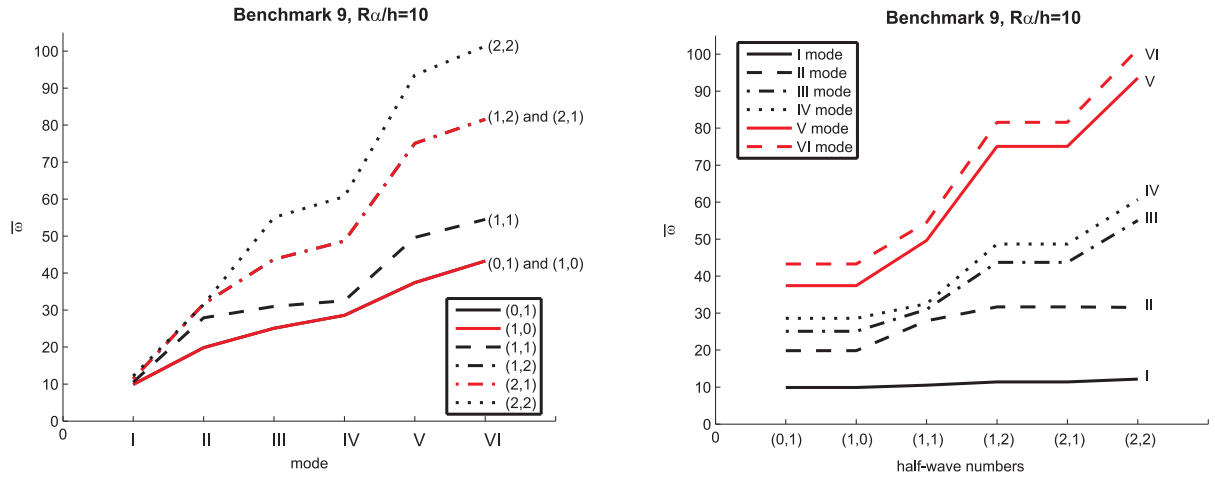


Figure 13: Benchmark 9, simply supported sandwich spherical shell panel with isotropic faces and thickness ratio  $R_\alpha/h = 10$ . No-dimensional circular frequencies versus mode order and half-wave numbers.